

**JAPAN INTERNATIONAL COOPERATION AGENCY  
GEOLOGICAL SURVEY OF ETHIOPIA**

**THE PROJECT FOR DEVELOPING  
COUNTERMEASURES AGAINST LANDSLIDES IN  
THE ABAY RIVER GORGE**

**SUPPLEMENTARY REPORT**

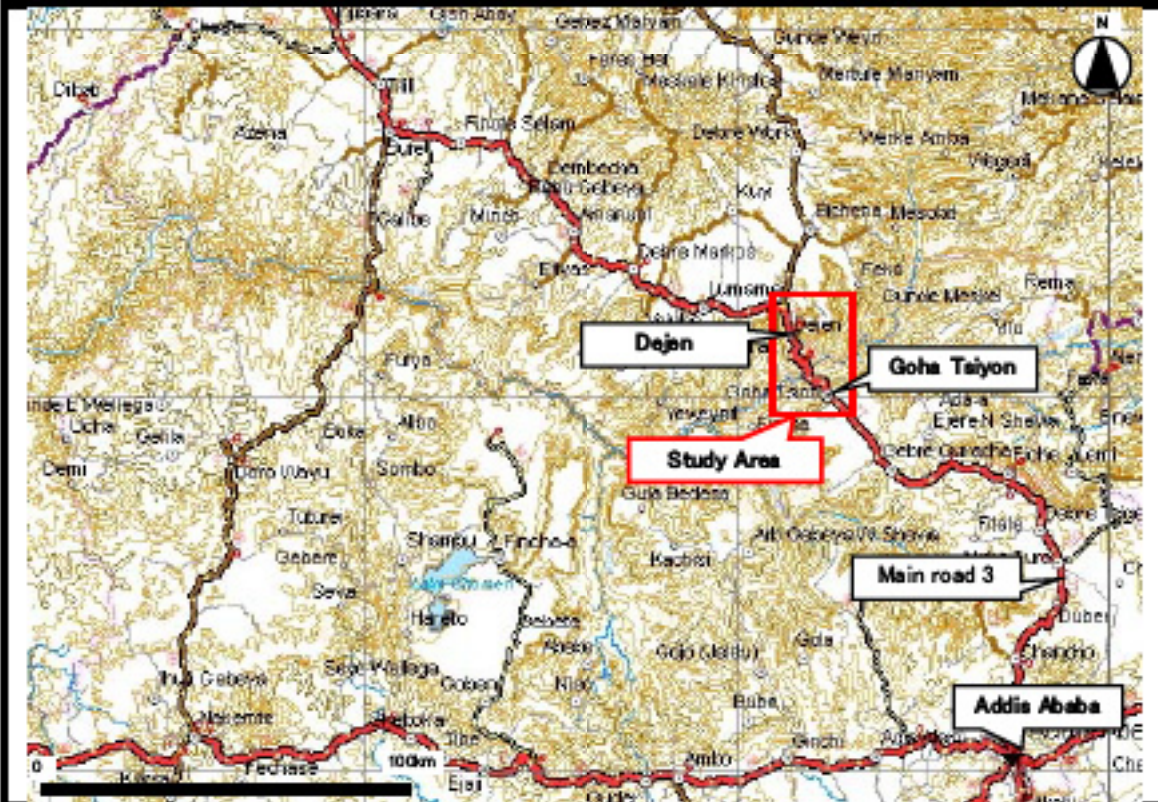
**March 2012**

**Kokusai Kogyo Co., Ltd.  
Japan Conservation Engineers Co.,Ltd.**

### Location of Study Area



### Detail Map



### Location Map

## Rate of Currency Translation

1 USD = 17.29 ETB  
= 77.73 JPY

1 ETB = 0.0578 USD  
= 4.4955 JPY

ETB: Ethiopia Birr

As of December 1<sup>st</sup>, 2011

# CONTENTS

Location Map  
Contents  
List of Figures  
List of Tables  
Abbreviations

	Page:
<b>1 Introduction.....</b>	<b>1-1</b>
<b>2 Landslide Survey .....</b>	<b>2-1</b>
2.1 Plan of survey .....	2-1
2.2 Drilling survey.....	2-3
2.2.1 Objective of drilling survey .....	2-3
2.2.2 Construction of access roads .....	2-3
2.2.3 Plan of drilling survey .....	2-4
2.3 Monitoring .....	2-7
2.3.1 Borehole Extensometer.....	2-7
2.3.2 Borehole Incliner .....	2-7
2.3.3 Groundwater Level Measurement .....	2-7
2.3.4 Electrical Resistivity Survey .....	2-7
2.4 Groundwater resistivity logging .....	2-16
2.4.1 Purpose .....	2-16
2.4.2 Principle.....	2-16
2.4.3 Measurement method .....	2-17
2.4.4 Instrumentation.....	2-18
2.4.5 Measure position.....	2-19
2.4.6 Analysis and judgment .....	2-19
2.4.7 Interpretation results.....	2-20
<b>3 Landslide Analysis and Interpretation.....</b>	<b>3-1</b>
3.1 Cross sectional interpretation .....	3-1
3.1.1 LS/00 .....	3-1
3.1.2 LS/05 .....	3-2
3.1.3 LS/27-28 .....	3-3
3.2 Monitoring data interpretation .....	3-5
3.2.1 LS/00 .....	3-5
3.2.2 LS/05 .....	3-6
3.2.3 LS/27 .....	3-6
3.2.4 LS/28 .....	3-6
3.3 Discussions on groundwater flow.....	3-8
3.4 Landslide mechanism and hydrogeological structure.....	3-10
3.4.1 Landslide section in each area and their hydrogeological characteristics.....	3-10
3.4.2 Summary of landslide mechanism and future works.....	3-12
<b>4 Technical Transfer.....</b>	<b>4-1</b>
4.1 Groundwater resistivity logging equipment.....	4-1

4.2	Laboratory soil test .....	4-3
4.2.1	General .....	4-3
4.2.2	Laboratory soil test equipment .....	4-3
4.2.3	Application for landslide analysis .....	4-7

## **Appendix**

Drilling logs

Core photos

Electrical Resistivity

Datasheets and analysis results of groundwater resistivity logging

Photos of groundwater resistivity logging in Abay Gorge

## List of Figures

	Page:
Figure 2.1.1 Location map of the landslide area	2-1
Figure 2.2.1 The location of access road (red line) and borehole points at (0 km)	2-4
Figure 2.2.2 The location of access roads (red line) and borehole points (27-28 km)	2-4
Figure 2.2.3 Photos of access road construction	2-6
Figure 2.3.1 Location and alignment of profile 1 (Goha Tsion site) and profiles 2 & 3 (Dejen site)	2-8
Figure 2.3.2 Location and alignment of profiles 4, 5 & 7 (Dejen site) and profile 6 (Dejen site)	2-9
Figure 2.3.3 Pole – Pole electrode array.	2-9
Figure 2.3.4 Resistivity section of profile 1 (Goha Tsion site)	2-11
Figure 2.3.5 Resistivity section of profile 2 (Dejen site)	2-11
Figure 2.3.6 Resistivity section of profile 3 (Dejen site)	2-12
Figure 2.3.7 Resistivity section of profile 4 (Dejen site)	2-13
Figure 2.3.8 Resistivity section of profile 5 (Dejen site)	2-14
Figure 2.3.9 Resistivity section of profile 6 (Dejen site)	2-14
Figure 2.3.10 Resistivity section of profile 7 (Dejen site)	2-15
Figure 2.4.1 Salt concentration and water resistivity	2-17
Figure 2.4.2 Groundwater Logging Zonde	2-18
Figure 2.4.3 Principle of groundwater resistivity logging to detect groundwater flow	2-20
Figure 3.1.1 Geological cross section in L/S00	3-1
Figure 3.1.1 Geological cross section in L/S05	3-2
Figure 3.1.1 Geological cross section in L/S27	3-3
Figure 3.1.1 Geological cross section in L/S28	3-4
Figure 3.3.1 Result of groundwater logging at borehole B00-16, with the pumping logging method	3-9
Figure 3.3.2 Result of groundwater logging at borehole B28-10, with the pumping logging method	3-9
Figure 3.4.1 Landslide section (BO-12 in L/S00 area)	3-10
Figure 3.4.2 Landslide section (BO-09 in L/S27 area)	3-11
Figure 3.4.3 Landslide section (BO-13 in L/S28 area)	3-11
Figure 3.4.4 Landslide section (BO-14 in L/S28 area)	3-12
Figure 4.1.1 Photos of the in-house seminar	4-2
Figure 4.1.2 Photos of the demonstration of the groundwater resistivity logging at EWTEC	4-2
Figure 4.2.1 Flowchart of soil survey for landslide prevention	4-4
Figure 4.2.2 Direct shear strength test	4-4
Figure 4.2.3 Compressive strength test machine for soil	4-5
Figure 4.2.4 One-dimensional consolidation test machine	4-5
Figure 4.2.5 Cone penetrometer	4-6
Figure 4.2.6 Compressive strength test machine for rock	4-6

## List of Tables

	Page:
Table 2.2.1 Drilling survey data .....	2-5
Table 2.3.1 Volume and technical settings of resistivity exploration .....	2-8
Table 2.4.1 Specifications of groundwater resistivity logging .....	2-19
Table 2.4.2 Result of groundwater resistivity logging .....	2-21
Table 3.2.1 Outline of the monitoring results .....	3-5
Table 3.3.1 Groundwater flowing investigation result through groundwater logging (in dry season).....	3-8
Table 4.1.1 Participants list on 2days seminar (19 and 20 December, 2011).....	4-1
Table 4.2.1 Cohesion and angle of internal friction of various landslides.....	4-7

## Abbreviations

C/P	Counterpart
CA	Capacity Assessment
DED	District Engineer Division
DEM	Digital Elevation Model
DRMC	District Road Maintenance Contractor
EMA	Ethiopian Mapping Agency
ERA	Ethiopian Roads Authority
GIS	Geographical Information System
GOE	Government of the Federal Democratic Republic of Ethiopia
GOJ	Government of Japan
GPS	Global Positioning System
GSE	Geological Survey of Ethiopia
IC/R	Inception Report
ITR(IT/R)	Interim Report
JCC	Joint Coordination Committee
JICA	Japanese International Cooperation Agency
L/S	Landslide
M/M	Minutes of Meeting
MM	Ministry of Mines
MME	Ministry of Mines and Energy
MoFED	Ministry of Finance and Economic Development
NGO	Non Governmental Organizations
NMSA	The Ethiopia National Meteorological Services Agency
PCM	Project Cycle Management
PDM	Project Design Matrix
PR (P/R)	Progress Report
S/C	Steering Committee
S/W	Scope of Work
The Project	Developing Countermeasures against Landslides in the Abay River Gorge
The Study Team	Japanese Study Team organized by JICA
WWIS	World Weather Information Service

# Chapter 1

---

---

*Introduction*



## 1 Introduction

This report covers the results of additional tasks on phase 3 for the Project on Developing Countermeasures against Landslides in the Abay River Gorge (hereinafter the Project) according to the Minutes of Meeting (hereinafter M/M) agreed upon between the Geological Survey of Ethiopia (hereinafter GSE), of the Federal Democratic Republic of Ethiopia (hereinafter Ethiopia) and the Japan International Cooperation Agency (hereinafter JICA) witnessed by the Ministry of Finance and Economic Development and Ethiopian Roads Authority (hereinafter ERA) of Ethiopia.

The Project launched at March 2010. The drilling survey, its analysis and the monitoring has been continuously conducting through two rainy seasons in the Project. In addition, the related technical knowledge has been transferred to counterpart (C/P) members in GSE. GSE has understand the flow of landslide investigation/analysis, the significance and the methodology and achieved a level which GSE can implement the investigation and the analysis by themselves.

However, the following equipment for landslide analysis was arrived at Ethiopia on phase 3 of the project. The JICA Study Team made technical transfer on this equipment to GSE.

- Groundwater resistivity logging equipment
- Laboratory soil test equipment (Direct shear strength test machine, Consolidation test machine, Cone penetrator for liquid limit, Compressive strength test machine for rock, Compressive strength test machine for soil)

The additional tasks of the Team on phase 3 are groundwater resistivity loggings on drilling survey and the subsequent laboratory soil test. The main tasks covered in the report are as follows.

- Technical supports and assistances for the drilling survey by GSE
- Technical supports and assistances for the groundwater resistivity logging
- Technical supports and assistances for the core sample identification on the drilling
- Procurement and management for the drilling survey
- Assistances for the installation of soil test equipment

This report is prepared and compiled mainly by GSE as a result of the technical transfer activity by the Team and also the efforts and challenges made by GSE C/P members.

# Chapter 2

---

*Landslide Survey*

## 2 Landslide Survey

### 2.1 Plan of survey

The targets are the areas prone to landslides in the Abay Gorge along main road 3 between Goha Tsiyon and Dejen (40.45 km). Based on topographic analysis using satellite photographs and site reconnaissance, we analyzed five landslide areas as the most dangerous areas to investigate and to take countermeasures, which have high risky landslide areas and the largest potential risk to roads (Figure 2.1.1).

L/S00 area  
L/S05 area  
L/S22 area  
L/S27 area  
L/S28 area

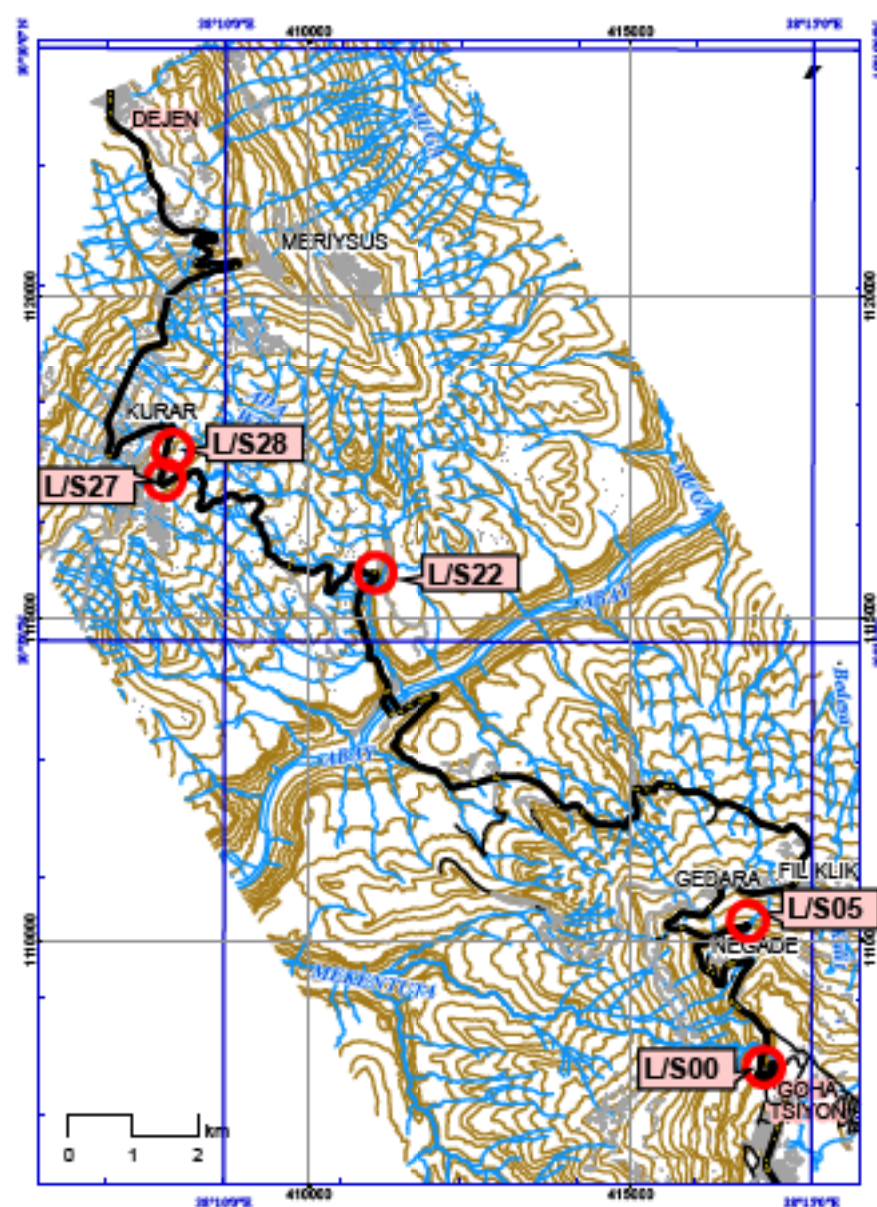


Figure 2.1.1 Location map of the landslide area

In the supplementary phase of the project remaining important works have been finalized providing additional information for complete analysis of the landslide areas. Out of 20 boreholes intended for the final phase of the investigation it has been possible to implement only 10 boreholes due to access problem. Access road has been cleared by own task force of the Geological survey of Ethiopia. Drilling was conducted from November 2011 to January 2012 after rainy season.

At the current stage 2 boreholes are added to the existing 5 boreholes at the LS/00 landslide site. Water level and inclinometer were installed in the boreholes for monitoring future movements. At LS27-28 landslide zone 8 boreholes are added at the site. Inclinometer, water level data, and borehole extensometer have been installed in the boreholes.

Geological core logging, borehole water level measurements were made during borehole drilling. Core samples have been photographed for archive and reference purpose with marks indicating depth graduated with 10cm interval. No laboratory samples have been obtained as all materials recovered from the boreholes are found almost identical to the previous samples where geological logging of the samples has been found sufficient. On the other hand the location of the boreholes further off from the road would have an important input for constraining displacement conditions for the landslide blocks identified early in the project.

Geophysical sounding for ground electrical resistivity was conducted in February, 2012. Total of 12 profiles were conducted in LS/27, LS/28, and LS/00 sites. Monitoring data acquisition has been acquired during the period and is planned to be continuously acquired every month.

## 2.2 Drilling Survey

### 2.2.1 Objective of drilling survey

The objective of this drilling survey is to implement a landslide monitoring study utilizing drilling points in agricultural fields along Abay gorge road. This drilling survey, except previously-implemented drilling survey, started in November of 2011.

So far, the Japanese expert team has implemented technical transfer relating to drilling survey and installing monitoring equipment etc. To check GSE C/P members' understanding, they were supervised and supported with:

- drilling work and installing monitoring equipment,
- negotiation to use agricultural land for access road installing,
- drilling core logging, and
- maintenance for monitoring equipment.

It confirmed that the technical transfer on drilling work is enough. Although the drilling survey had made the progress, the difficulty of drilled faced in the layer of boulder stone on B27-33 and up to the planning depth couldn't be drilling due to stacking the drilling bit in the period of 5th December to 8th December. Then another borehole shifted from 1 meter to the first tried borehole was drilled. All of the drilling works were completed in the beginning of January 2012 (shown in Table 2.2.1 & Figure 2.2.4).

### 2.2.2 Construction of access roads

Planned drilling points are in agricultural fields; therefore construction of access roads is needed.

The drilling survey started in November 2011 is delayed due to problems with bulldozer procurement. The bulldozer is needed for developing agricultural land to be acquired for survey sites and access roads.

ERA (Ethiopian Road Authority) initially agreed to arrange the bulldozer. ERA could not follow through with this; therefore GSE counterparts organized the procurement of the GSE bulldozer in the beginning of November 2011.

Moreover, land-use permits are needed to acquire the agricultural land for access roads. The GSE counterparts will negotiate to obtain the permits. Most land in Ethiopia is government owned. So the negotiations were with land users (and/or land owners, Woreda Officer) for the land acquisition.

The fields were planted with sorghum, corn, maize and teff, and it was the pre-harvest period.

Access road routes were planned and arrangements made, taking due consideration to minimize land damage, before the drilling survey started (shown in Figure 2.2.3).

## 2.2.3 Plan of drilling survey

The access roads layout and the borehole points for the drilling survey are shown in Figure 2.2.1- Figure 2.2.2. The drilling survey data is mentioned in Table 2.2.1.

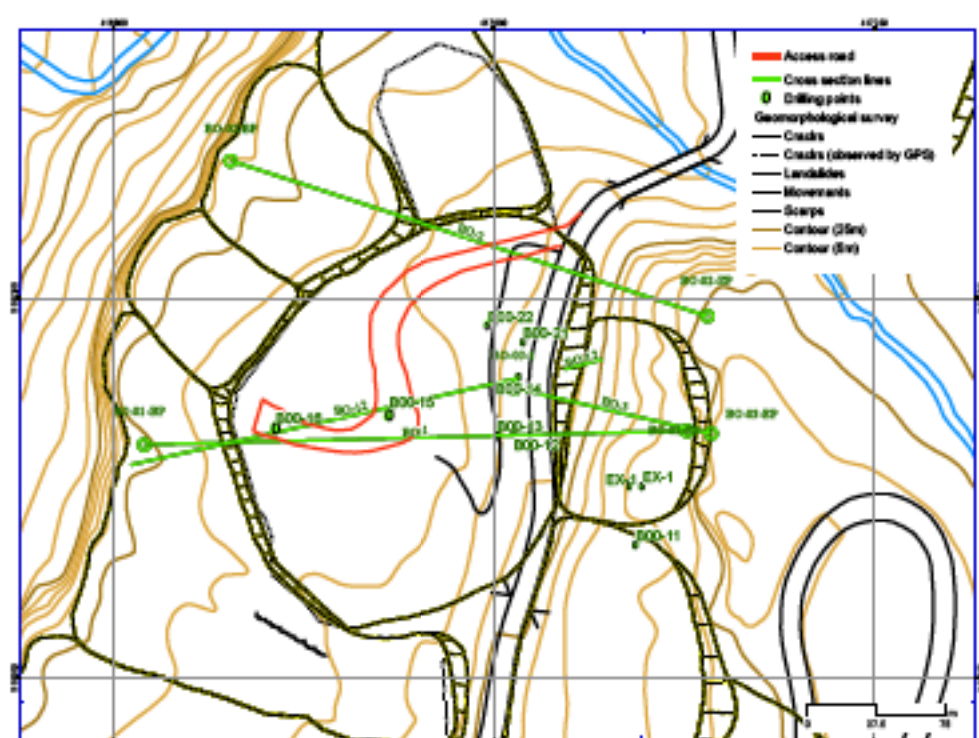


Figure 2.2.1 The location of access road (red line) and borehole points at (0 km)

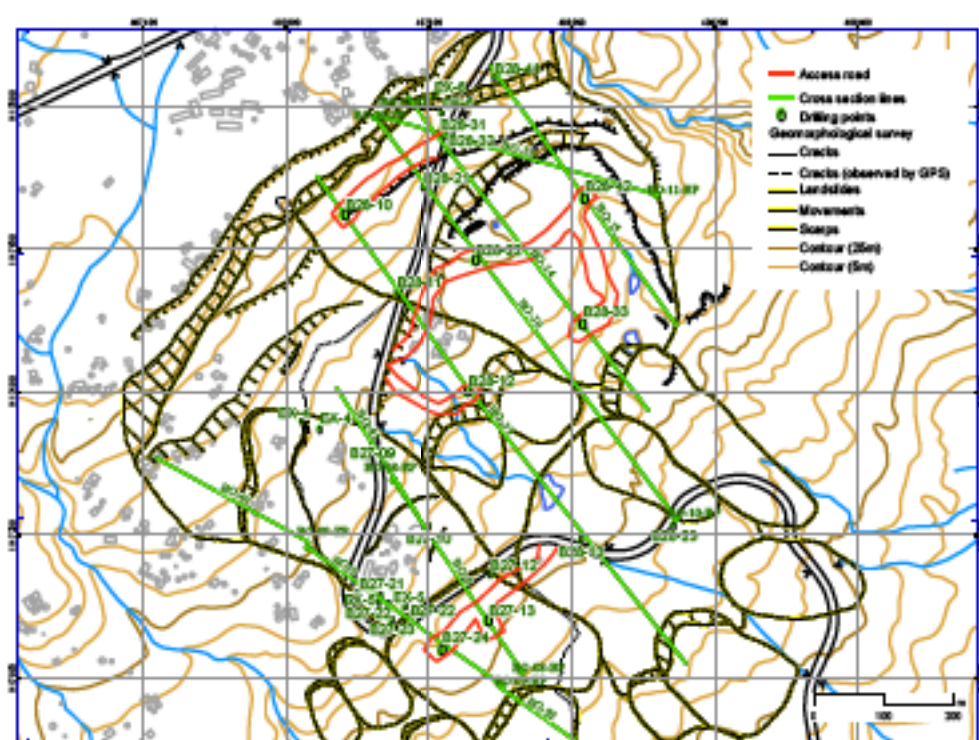


Figure 2.2.2 The location of access roads (red line) and borehole points (27-28 km)

Table 2.2.1 Drilling survey data

No.	Location	Name	Drilling survey		Monitoring installation			Preparation			GPS location			water level(m)	working period (2011/2012)
			No.	Core drilling (m)	Automatic water level meter (m)	Borehole inclinometer (m)	Borehole extension meter (m)	C. construction of access road (m)	X	Y	Height(m)	X	Y		
1	00+800 ~ 01+100	L/S00	B00-15	30		30		130	416943	1108133	2367	-10.20	6th/Jan.	3rd/Jan.	6th/Jan.
			B00-16	25	2.5			10	416890	1108121	2731	-11.50	3rd/Jan.	30th/Dec.	3rd/Jan.
2	27+500 ~ 27+900	L/S27	B27-13	25			25	60	407879	1117078	1697	-12.20	29th/Dec.	24th/Dec.	29th/Dec.
			B27-24	25	2.5			25	407816	1117050	1708	-18.15	24th/Dec.	19th/Dec.	23rd/Dec.
3	28+000 ~ 28+700	L/S28	B28-10	40	40			120	407686	1117640	1783	-19.50	21st/Nov.	16th/Nov.	19th/Nov.
			B28-12	30			30	175	407859	1117400	1735	-8.10	16th/Dec.	14th/Dec.	17th/Dec.
			B28-22	30	30			140	407867	1117578	1746	-14.10	25th/Nov.	21st/Nov.	24th/Nov.
			B28-33	30	30			90	408015	1117496	1727	-17.15	13rd/Dec.	8th/Dec.	13th/Dec.
			B28-42	30			30	150	408027	1117664	1740	-5.00	2nd/Dec.	26th/Nov.	2nd/Dec.
			Total sites	9	5	1	3	9							
Total length (m)			265	150	30	85	900								



Construction of access road for drilling point B28-33  
(sorghum field)



Construction of access road for drilling point B28-12  
(sorghum field)



Construction of access road for drilling points B27-13  
and B27-24 (maize field)



Construction of access road for drilling points B00-15  
and B00-16 (teff field)

Figure 2.2.3 Photos of access road construction



## 2.3 Monitoring

A summary of the mechanism of the installed monitoring devices during the supplementary phase of the project is given in the subsequent sections. To identify trigger/motion mechanisms of landslides, measurements were made with extensometers. These were installed along the direction of landslide movement and along each survey line to measure the amount of expansion/contraction in cracks and subsidence. To measure movement of a slip surface in the ground, borehole extensometers were installed at drilled borehole points.

The groundwater level in boreholes is measured continuously by groundwater level meters, the correlation between groundwater level and precipitation is investigated, and also the relationship between groundwater level and landslide activity is considered. The purpose of main slip surface survey is to determine the position of the slip surface. A borehole inclinometer measurement is one of the most important factors to determine it, and also to quantitatively grasp the displacement of a landslide. Monitoring data has been acquired to cover the entire time lapse from rainy season up to the current.

### 2.3.1 Borehole Extensometer

To measure movement of a slip surface in the ground, borehole extensometers were installed at drilled borehole points. Three borehole extensometers have been installed in the LS/27 and LS 28 landslide zones.

### 2.3.2 Borehole Inclinometer

The purpose of main slip surface survey is to determine the position of the slip surface. A borehole inclinometer measurement is one of the most important factors to determine it, and also quantitatively grasp the displacement of a landslide. Inclinometer has one disadvantage in that it only renders use until one of multiple occurring slip planes obliterate its entire length. After closing of the pipe no more measurement can be taken hence strain gauges are usually suitable for multiple depths of slip plane occurrence. One inclinometer casing has been installed in one borehole at LS/00 Landslide area in the last stage of the investigation. Although no movement is expected until the next rain event it can serve to compare the activity of the landslide before and during rainy season.

### 2.3.3 Groundwater Level Measurement

The groundwater level in boreholes is measured continuously by groundwater level meters, the correlation between groundwater level and precipitation is investigated, and also the relationship between groundwater level and landslide activity is considered. Five water level meters have been installed, one at LS/00 landslide zone and four at LS/27 and LS 28 landslide zones.

### 2.3.4 Electrical Resistivity Survey

The second phase resistivity investigation is made to estimate horizontal continuity of weathered and permeable layers in landslide slopes, and delineate faults from the two-dimensional distribution of ground resistivity, as well as to prepare the basic data for groundwater drainage works.

Here, in the two-dimensional resistivity exploration the electric potential is measured in high density using electrodes arranged at 5 meters interval on a traverse line. This exploration is used to obtain a resistivity distribution that satisfies the measured potential data through an inverse analysis of the acquired potential data using Geo soft “Oasis Montaj” software.

**a. Volume of work**

Table 2.3.1 Volume and technical settings of resistivity exploration

# of traverse line (profile)	Site	Profile length (m)	Electrode interval (m)	Max. depth (m)	Number of observation (points)
Profile 1	Goha Tsion	160	5	40	32
Profile 2	Dejen	460	5	40	92
Profile 3 (Upper)	Dejen	80	5	40	16
Profile 3 (Lower)	Dejen	460	5	40	92
Profile 4 (Upper)	Dejen	195	5	40	39
Profile 4 (Middle)	Dejen	435	5	40	87
Profile 4 (Lower)	Dejen	185	5 <td 40	37	
Profile 5 (Upper)	Dejen	150	5	40	30
Profile 5 (Lower)	Dejen	130	5	40	26
Profile 6 (Upper)	Dejen	460	5	40	92
Profile 6 (Lower)	Dejen	140	5	40	28
Profile 7	Dejen	215	5	40	43

**b. Survey locations**

The survey area is divided in to two sites namely, Goha Tsion and Dejen. At Goha Tsion site only one profile and at Dejen site six profiles were conducted.

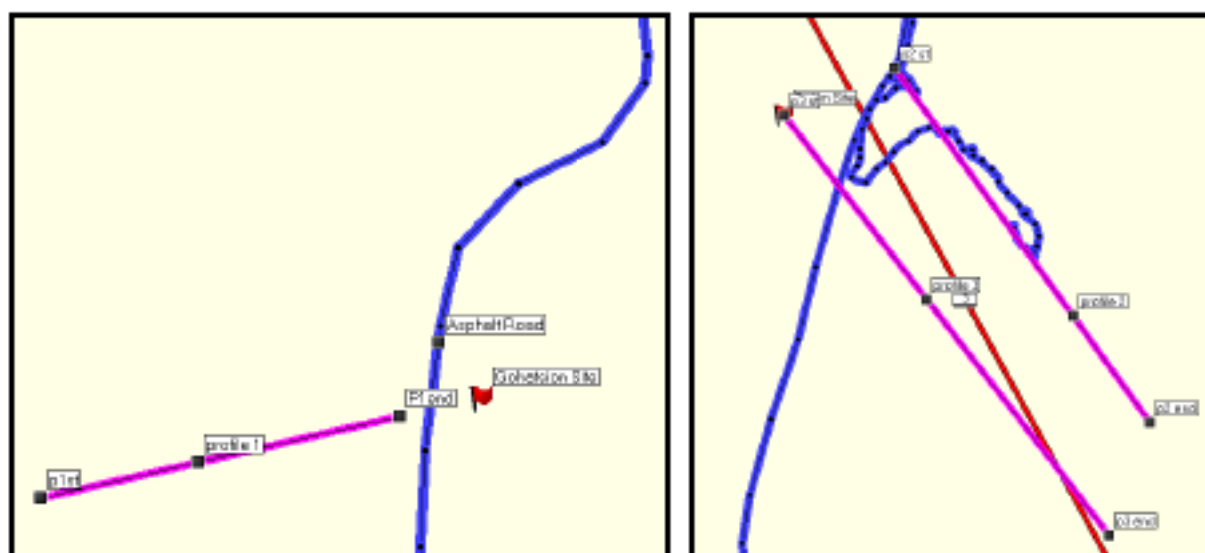


Figure 2.3.1 Location and alignment of profile 1 (Goha Tsion site) and profiles 2 & 3 (Dejen site)

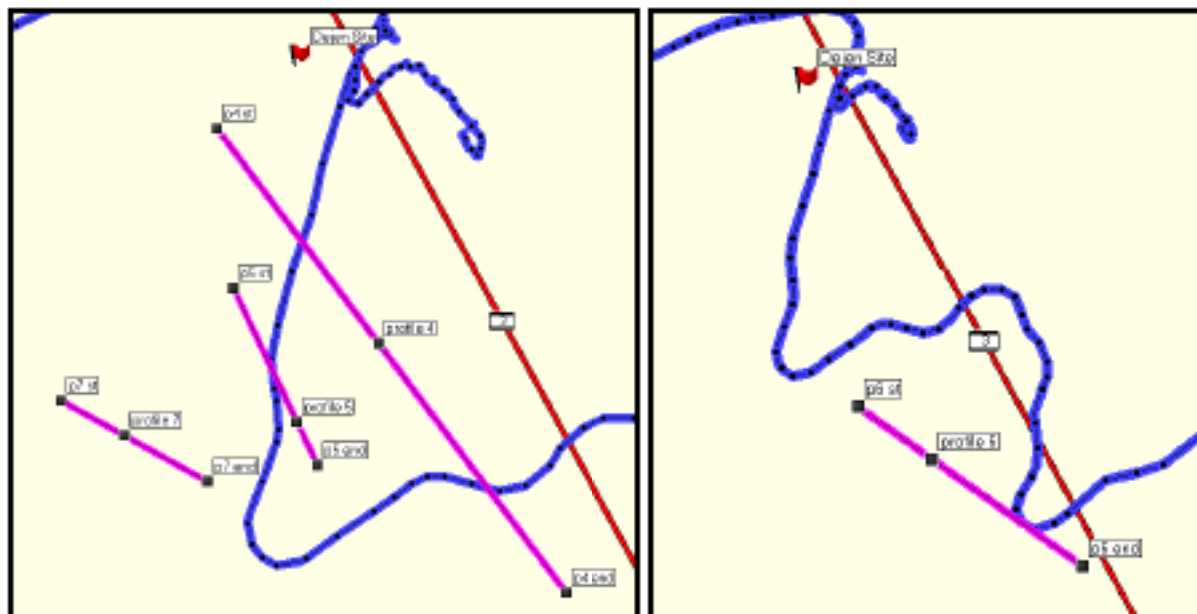


Figure 2.3.2 Location and alignment of profiles 4, 5 & 7 (Dejen site) and profile 6 (Dejen site)

### c. Equipment

During survey the following equipments were utilized.

- SuperSting R1/IP manufactured by Advanced Geosciences, Inc.
- Electrode bars made of stainless steel
- Electric cable, car battery
- GPS for locating the exact coordinates of survey points.

### d. Measuring Method

For this project we used a manual mode pole-pole measurement method. Figure 1.6 shows a circuit diagram of pole - pole electrode array where  $I$  is the current passing through electrodes  $C$  and  $C_{\infty}$ ,  $V$  is the potential between electrode at  $P$  and  $P_{\infty}$  respectively.

By keeping position of the current electrode constant and varying the potential electrode position for every 5m the amount of potential between  $P$  and  $P_{\infty}$  is measured. After eight measurement of potential has been taken the position of the current electrode is shifted to 5m and the procedure repeats itself until the profile ends. The apparent resistivity  $\rho$  can be obtained from the following equation using the potential theory of semi-infinite medium.

$$\rho = 2\pi a \times V/I \text{ (}\Omega\text{-m)}$$

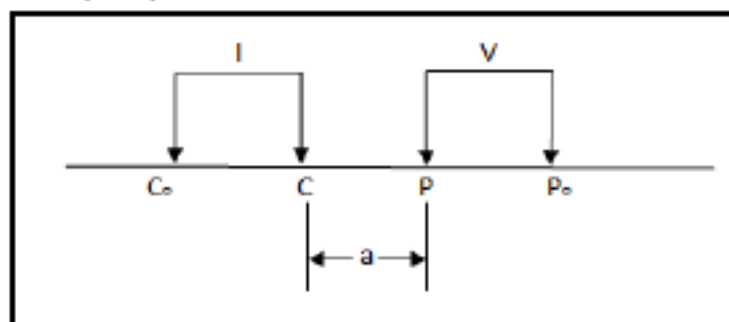


Figure 2.3.3 Pole - Pole electrode array.

### **e. Analysis Method**

An inverse analysis (inversion) is made using the nonlinear least-squares method to obtain a color underground resistivity sectional view from a great deal of measured potential data. For analyzing the result, we used 2D Earth Imager of AGI.

Procedures for analysis and calculation are as follows.

- 1) Create an initial model of resistivity distribution using the measured data.
- 2) Obtain a logical potential based on the resistivity distribution using the finite element method.
- 3) Calculate the difference (residual) between the measured potential and the logical potential.
- 4) Calculate the logical potential while modifying the initial model so that the residual becomes minimal.
- 5) Repeat steps 2) to 4) until the residual converges to gain a final resistivity model.

### **f. Analysis standards**

In general, the ground resistivity shows the following trends.

- The resistivity value of pelitic origin rocks is small while the resistivity value of rocks consisting of coarse grained minerals such as granite is large.
- The resistivity value of weathered and altered rocks is smaller than that of unweathered rocks with the same geology.
- The resistivity value decreases as water content increases.
- The resistivity value of fault and crush area or altered area is smaller than the resistivity value of their peripheries.
- The resistivity value of gravel layer is larger than that of clay layer.

Although these trends are seen, the ground resistivity generally depends on many factors such as content of conductive minerals (including clay mineral), porosity, water content and saturation, water quality of pore water (resistivity), and temperature. Furthermore, the resistivity simply indicates lithofacies changes in the same geological layer/rock, degree of weathering/hydrothermal alteration, and water content status in many cases in addition to differences in geological layers and rocks.

### **g. Analysis results**

#### **g.1 Resistivity section of profile 1**

For our analysis, we classify the resistivity section of profile 1 (Figure 1.7) in to three major parts. The first part of the profile ranges from 0 to 85 station with apparent Resistivity value of 62 – 100  $\Omega$ -m. This part covers nearly half of the profile.

The second part ranges from station 35 to 135 with apparent resistivity of 14 – 49  $\Omega$ -m indicating the presence of a relatively saturated and weathered layer.

The third layer covers stations from 105 – 160 with a relatively high apparent resistivity value of 159 -533  $\Omega$ -m. From the field observation, this area is covered by basalt boulders.

From geo hazard point of view, such geological formation is highly prone to landslide phenomenon.

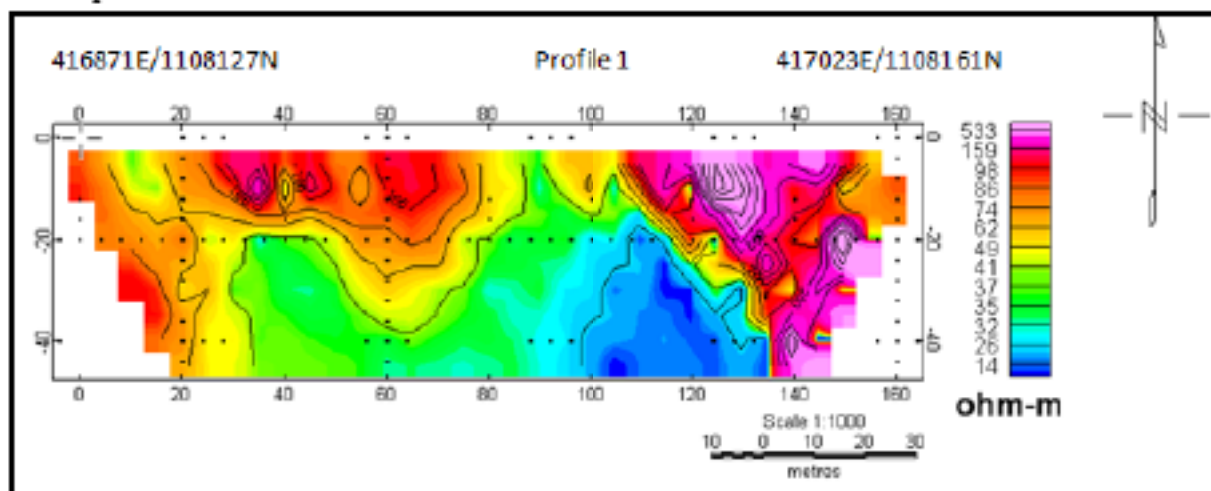


Figure 2.3.4 Resistivity section of profile 1(Goha Tsion site)

### g.2 Resistivity section of profile 2

The resistivity section along profile 2 can be classified in to two parts.

Accordingly, the first part ranges from station 0 to 300 with apparent resistivity value of 22 - 53  $\Omega$ -m. However, corresponding to station 45, 160 and 220, fracture/saturated zone is observed.

This part comprises the relatively elevated area hence; the observed high resistivity value might be due to the less moisture content in the underlying layers.

The second part of resistivity section ranges from station 240 to 460 with apparent resistivity value of 11 – 20  $\Omega$ -m likely to be the response of saturated and weathered layer.

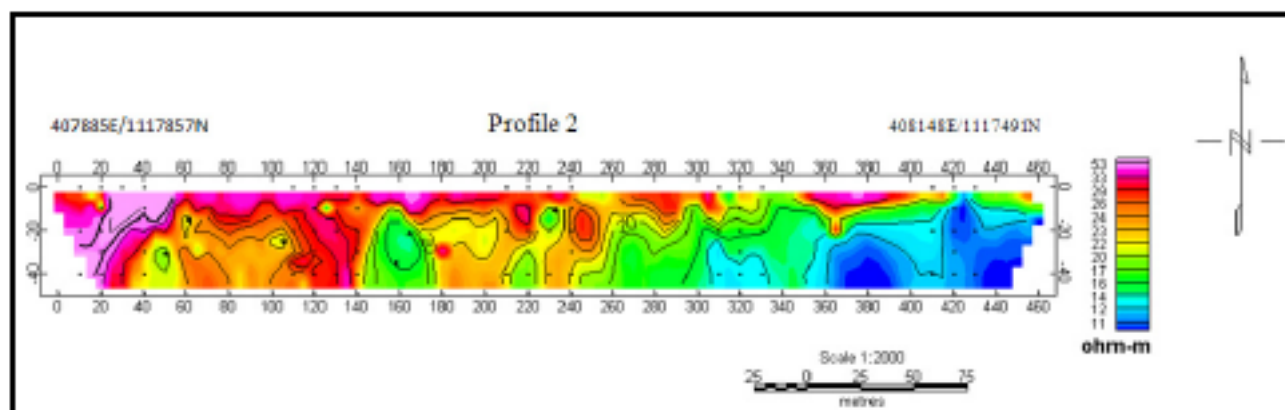


Figure 2.3.5 Resistivity section of profile 2 (Dejen site)

### g.3 Resistivity section of profile 3

This profile is divided into two parts by the road. Therefore, we consider left part of the

profile as the upper and the right side as lower part of the profile.

#### The upper part

The upper part of profile 3 can be partitioned in to two according to its resistivity distribution. The first part ranges from station 0 to 60 characterizing a relatively high resistivity value of 39 – 74  $\Omega$ -m due to the less moisture content. It is a relatively elevated part the profile.

The second part ranges from station 25 to 80 with resistivity of 18 – 29  $\Omega$ -m. It can be considered as fractured and saturated part of the profile.

#### The Lower part

The overall length of lower part is 460 meters and from the electrical resistivity distribution point of view, it can be divided in to three parts.

The first part which ranges from station 0 to 240 is characterized by 19 – 34  $\Omega$ -m apparent resistivity value. However, between stations 80 and 180, the section is marked with a relatively low apparent resistivity value of 10 – 17  $\Omega$ -m.

The second part ranges from station 200 to 420 with apparent resistivity of 10 - 16  $\Omega$ -m indicating the highly saturated part of the section.

The third part comprises stations between 360 – 460 with a relatively higher apparent resistivity value (19 – 24  $\Omega$ -m) compared with the underlying layer. The observed resistivity might be due to embankment of the road towards end of the profile.

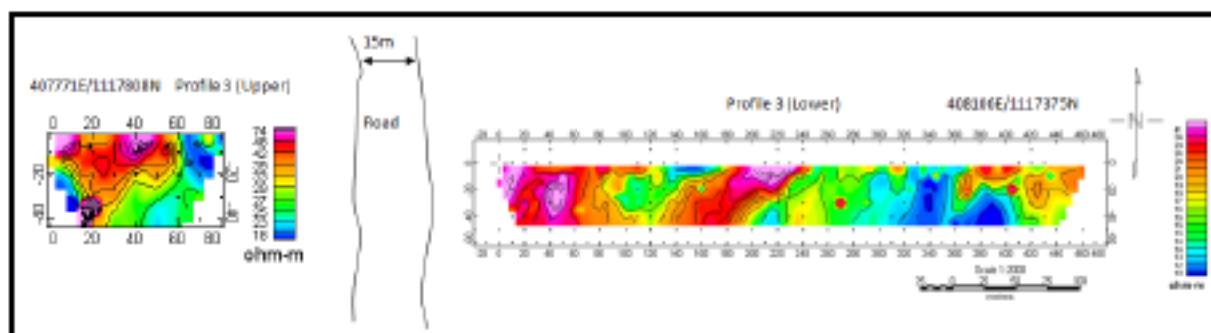


Figure 2.3.6 Resistivity section of profile 3 (Dejen site)

#### **g.4 Resistivity section of profile 4**

Profile 4 is crossed twice by the road and divided in to three parts namely, the upper, middle and lower therefore; we shall analyze each of them separately.

#### The upper part

The upper part of profile 4 can be classified in to two from which the first part ranges from station 0 to 120 is characterized by 17 – 79  $\Omega$ -m resistivity value. However, between stations 40 and 90, the section is marked with relatively low resistivity value of 14  $\Omega$ -m which might be due to fractured nature of the layer.

The second part ranges from station 90 to end of the profile with resistivity ranging between 14 - 16  $\Omega$ -m possibly a response of a saturated/fractured layer. However, within this part of

the section a relatively high resistive bodies ( $79 \Omega\text{-m}$ ) are delineated which might be due to basalt boulders.

#### The middle part

The middle part of profile 4 can be divided in to three parts, from which the first part ranges from station 0 – 180 with resistivity value of  $19 - 34 \Omega\text{-m}$  indicating the dry nature of the section.

The second part comprises stations between 165 – 410 with a relatively lower resistivity value ( $11 - 13 \Omega\text{-m}$ ). The observed resistivity might be due to the highly saturated nature of the section as the pond was observed there during field traverse.

The third part ranges from station 350 to 440 (end of the profile) showing an increment in resistivity from the second one ( $15 - 24 \Omega\text{-m}$ ), which might be the response of road embankment material.

#### The lower part

The lower part of profile 4 can be divided in to two parts, from which the first part ranges from station 0 – 100 with resistivity value of  $14 - 19 \Omega\text{-m}$  indicating the dry nature of the section, even though corresponding to station 40, the highly fractured nature of the section is exposed to the surface with less resistivity value of  $12 \Omega\text{-m}$ .

The second part comprises stations between 80 – 180 with a relatively lower resistivity value of  $12 - 13 \Omega\text{-m}$ . The observed low resistivity might be due to the highly fractured and saturated nature of the section.

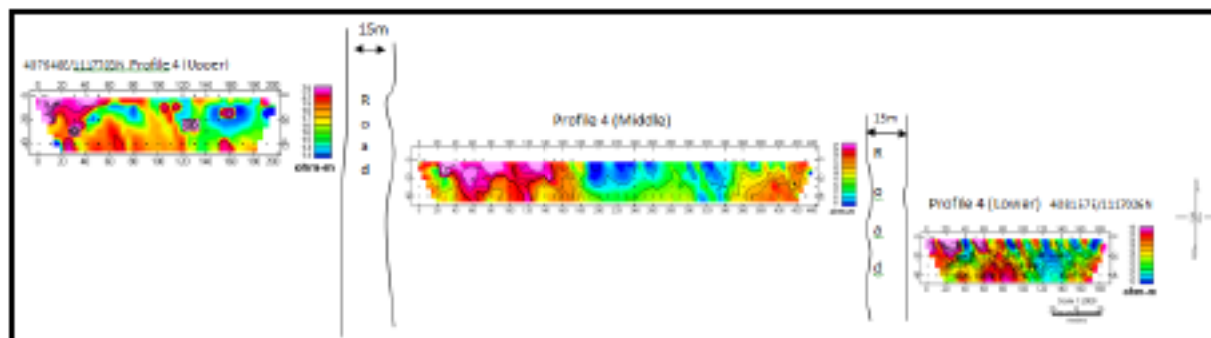


Figure 2.3.7 Resistivity section of profile 4 (Dejen site)

### **g.5 Resistivity section of profile 5**

Profile 5 is crossed once by the road and divided in to two parts namely, the upper and lower therefore; we shall analyze each of them turn by turn.

#### The upper part

The upper part of profile 5 can be divided in to two. Here, the first part ranges from station 0 to 150 is characterized by  $7 - 12 \Omega\text{-m}$  resistivity value. This part comprises the top weathered and saturated layer with thickness of about 22 meters. This part of profile crosses the sugar cane plantation.

The second part also ranges from station 0 to end of the profile with resistivity of between 14

- 20  $\Omega$ -m. This part comprises the bottom and relatively consolidated layer with less moisture content than the top layer.

#### The lower part

The lower part of profile 5 can be divided in to two. Here, the first part ranges from station 10 to 130 is characterized by 21 – 28  $\Omega$ -m resistivity value. This part comprises the top dry and weathered layer with thickness between 20 - 40 meters.

The second part ranges from station 0 to 30 and from 50 to 120 with resistivity between 16 - 19  $\Omega$ -m. comprising the bottom and relatively saturated layer.

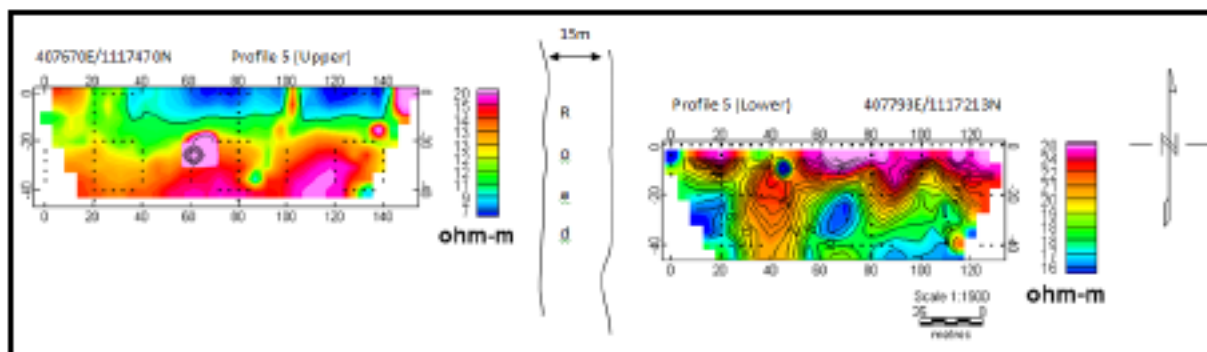


Figure 2.3.8 Resistivity section of profile 5 (Dejen site)

#### **g.6 Resistivity section of profile 6**

Profile 6 is crossed by the road and divided in to two parts namely, the upper and lower therefore; we shall interpret each of them turn by turn.

#### The upper part

The upper part of profile 6 can be divided in to two. Accordingly, the first part ranges from station 0 to 380 and from 380 to 460 characterized by 24 – 39  $\Omega$ -m resistivity. This part comprises the top dry and resistive layer. Within station interval of 0 and 270, it overlies on a relatively saturated second layer with resistivity value of 13 – 18  $\Omega$ -m and to the contrary, within station interval of 380 and 460, it is overlain by the saturated layer of thickness of about 30 meters.

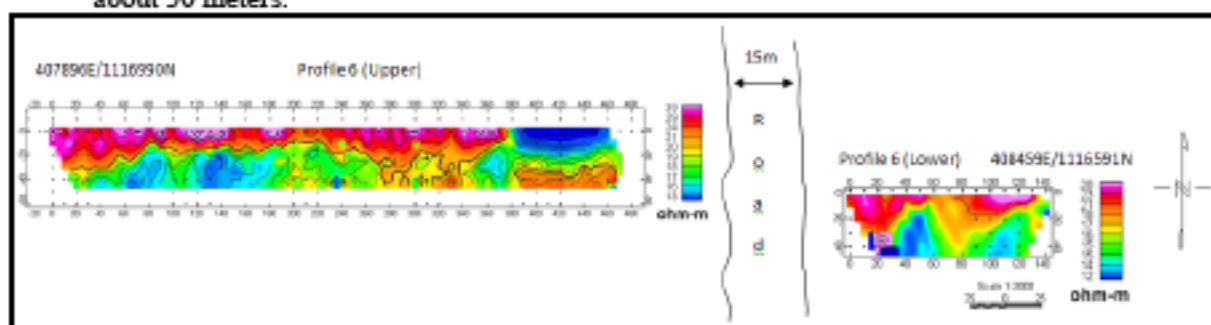


Figure 2.3.9 Resistivity section of profile 6 (Dejen site)

#### The lower part

The lower part of profile 6 can be divided in to two. Here, the first part ranges from station 0 to 140 characterized by 18 – 38  $\Omega$ -m resistivity value. This part comprises the top dry and relatively more resistive layer with thickness between 5 - 35 meters.



The second part ranges from station 10 to 140 with resistivity between 12 - 15  $\Omega$ -m. comprising the bottom and relatively saturated layer.

#### g.7 Resistivity section of profile 7

The resistivity section along profile 7 can be classified in to two parts.

Accordingly, the first part ranges from station 0 to 40, 45 to 140 and 185 to 215 with resistivity value of 13 - 22  $\Omega$ -m. This part comprises the top dry and more resistive part of the section.

The second part of resistivity section ranges from station 10 to 75 and from 100 to 210 with app. resistivity of 9 - 12  $\Omega$ -m likely to be the response of saturated and weathered layer.

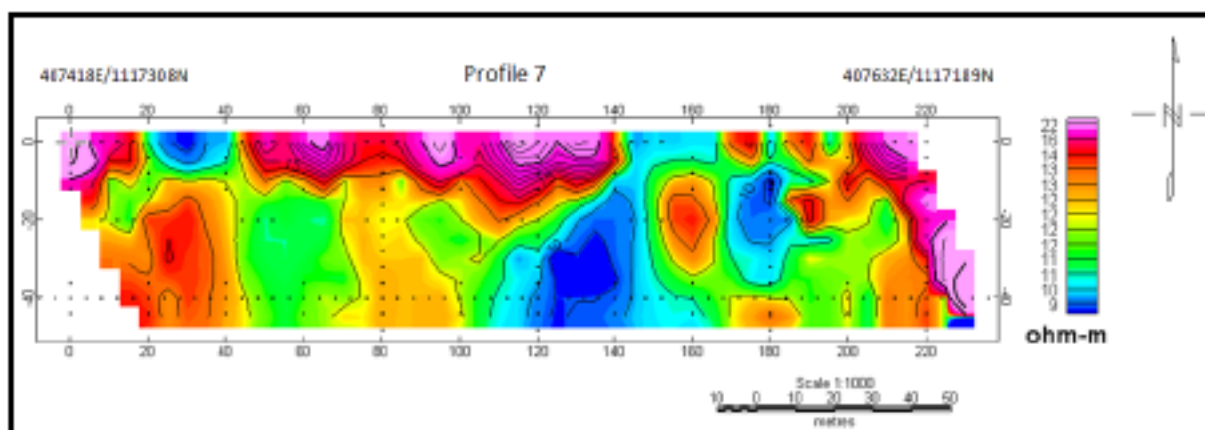


Figure 2.3.10 Resistivity section of profile 7 (Dejen site)

## 2.4 Groundwater resistivity logging

### 2.4.1 Purpose

Groundwater resistivity logging is conducted for the purpose to understand the position of the groundwater flowing, flowing situation and change of the groundwater through the measurement of the resistivity of groundwater in borehole. The followings are the main purposes.

- To confirm the groundwater flowing layer related to the landslide;
- To estimate the pressure head of each groundwater flowing layer;
- To estimate the position of the sliding surface

### 2.4.2 Principle

In general, the electrical resistivity of groundwater is high because there is little dissolved substance and suspended solids in it. The groundwater flowing into a borehole has the same property. When a small quantity of electrolyte, generally salt is dissolved into the water in borehole, the electrical resistivity will decrease obviously. When fresh groundwater flows into the electrolyte solution, the electrical resistivity will become higher again because the electrolyte solution will be diluted by the fresh water. Figure 2.4.1 shows the relationship. In this figure, abscissa presents the concentration of salt in water, while the axis of ordinate presents the resistivity of the water, which is calculated as electrical resistivity of an electric conductor in unit cross section and unit length, and the dimension is  $k\Omega \cdot cm$ . In Figure 2.4.1 (a), the scale is shown in logarithm, while in Figure 2.4.1 (b), it is shown in even interval graduation.

In the measurement process, electrolyte is dissolved into the groundwater in borehole at first to decrease the electrical resistivity of the water in the borehole. Then, continuous measurements are made in a certain time interval. If there is fresh water flowing into the borehole at certain depth, the electrical resistivity will become larger because the concentration of electrolyte is diluted. On the contrary, at another depth where there is no inflowing of fresh groundwater, the electrical resistivity will not change because the concentration of the electrolyte has not been affected by fresh groundwater inflow. According to the changing patterns of the electrical resistivity in the borehole groundwater, the groundwater distribution can be prospected. This method is called as groundwater resistivity logging.

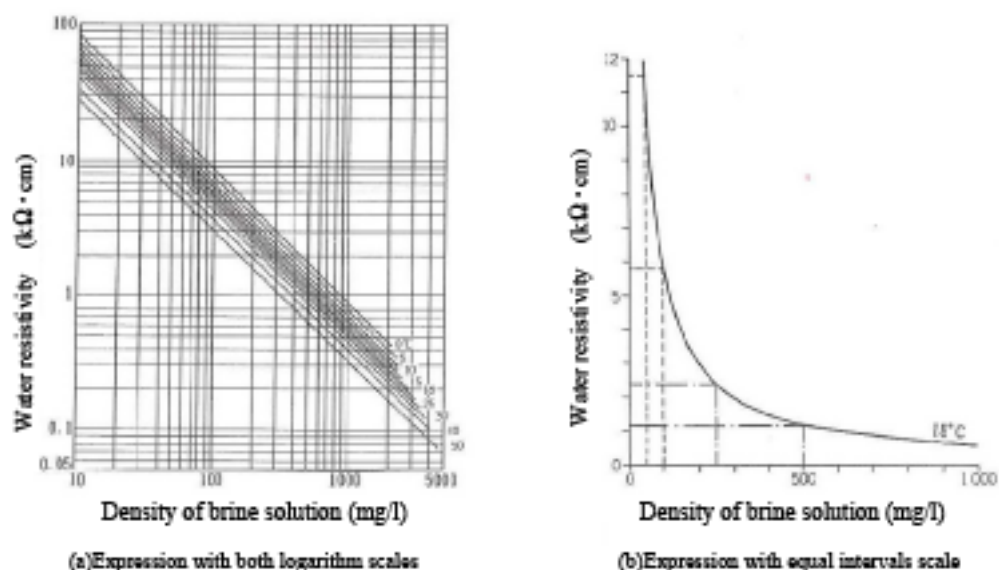


Figure 2.4.1 Salt concentration and water resistivity

### 2.4.3 Measurement method

The measurement is conducted by measuring the electrical resistivity distribution along the borehole depth direction at certain times repeatedly. Concretely saying, the first measurement should be conducted before the salt is added in the borehole to get the background value (B.G. value) when the groundwater is at the natural condition. Then as soon as the salt is dissolved into the groundwater in borehole, the second measurement should be conducted to get the highest value of the resistivity. After the second measurement, continuous measurements should be conducted for at least two hours at a certain time interval. Furthermore, the measurement should be conducted at every 0.25m depth-wise. The following introduces two methods used in the measurement.

#### a. Natural water level method

- Measure the water level in the borehole.
- Measure the background water of the resistivity in the borehole in natural state. In this measurement, if there is obvious difference in the resistivity value along the depth direction along the borehole, the borehole should be washed with pure water. Then wait until the water level in the borehole becomes stable, and measure the water level in the borehole.
- Dissolve the salt in the groundwater in the borehole.
- Measure the resistivity of the groundwater in the borehole continuously at a certain time interval while maintaining the natural water level at the constant level. The following shows an example for measuring interval for reference. When the resistivity of water recovering is quick, the time interval can be shortened in order to grasp the whole situation of the resistivity change.

Example: after the salt is added (set the time as 0), the measurements are conducted at 5, 10, 20, 30, 45, 60, 90, 120 minutes

#### b. Pumping method

- Measure the water level in the borehole.
- Measure the background water of the resistivity in the borehole. Occasionally, salt used in the natural water level method is left in the borehole. Nonetheless, washing process can be omitted in the pumping method.
- Dissolve the salt in the borehole.
- Measure the resistivity at the natural water level as soon as the salt is added in the borehole.
- Start the pumping as soon as the measure is conducted. The continuous measurements are also conducted at the certain time interval while keeping the pumping at a constant pace. The pumping and measurement process should continue until it is confirmed that groundwater has flowed into the borehole near the sliding surface, or the final target groundwater level (generally a little bit higher than the sliding surface) has been reached.
- Although the measurement time can be set as the same as that used in natural water level method, it is desirable to continue the measurement until the groundwater inflow to the borehole near the sliding surface is confirmed.

It should be noted that when logging the resistivity, the natural water level method measurement should be conducted before the pumping method.

#### 2.4.4 Instrumentation

Measuring Instrument;  
SSE-KYOWA KCM-200C

Zonde; GWL-P(60m)

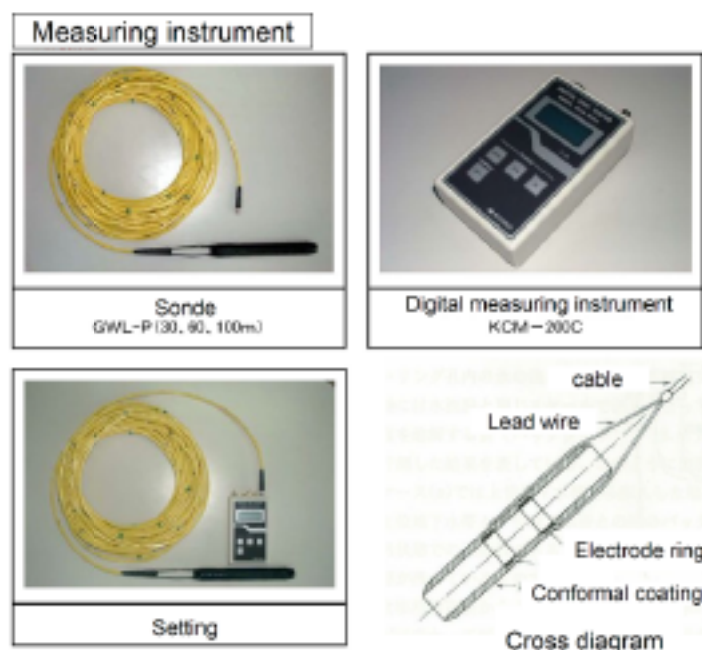


Figure 2.4.2 Groundwater Logging Zonde

## 2.4.5 Measure position

Table 2.4.1 shows the position and depth of the groundwater resistivity loggings which have been conducted.

Table 2.4.1 Specifications of groundwater resistivity logging

Location	Borehole Number	Core drilling (m)	Groundwater level(m)	Measured depth (m)	Measured date
L/S 00	B00-16	25	11.5	11.75-25.75	5 Jan.2012
L/S 05	B05-31	35	23.5	23.75-35.00	3 Jan.2012
L/S 27	B27-24	25	21.6	21.75-24.00	27 Dec.2011
L/S 28	B28-10	40	31.3	31.50-39.50	26 Dec.2011
	B28-33	30	23.1	23.25-28.00	28 Dec.2011

## 2.4.6 Analysis and judgment

In the relationship curve of depth and water resistivity, vertical distribution of water resistivity obtained by adjusting measurement time allows the groundwater flow and its conditions to be interpreted.

- Groundwater afflux layer: It refers to the inflow of the groundwater which can be confirmed using the natural water level method. Case- b in Figure 2.4.3 is the example.
- Pressured groundwater: The inflow section of groundwater detected through the pumping method which affects the groundwater pressure. When groundwater layer is detected in the pumping method, it is estimated that the groundwater layer is under pressure, and it is judged as pressured groundwater.
- Leakage of groundwater: It refers to the end point of vertical flow which including ascending flow and descending flow in the borehole, and the point where the flowing rate of vertical flow starts to decrease. This phenomenon occurs when in-flowed groundwater from the flowing-in layer leaks back to the surrounding ground again after the vertical flowing in the borehole. The leakage point indicates the path of groundwater, and it should be weak in geological structure. Sometimes it can be considered that the sliding surface has been formed near the leakage position. Case-c and case-d are the examples.
- Un-afflux layer : In this layer, there is no change detected after the salt is added. →case-a

In Figure 2.4.3, HW indicates the pressure head of an aquifer layer at a certain depth, while HW is the height of water level from the aquifer layer measured in borehole. Generally, it is considered that the flowing of groundwater is weak in the natural water level method.

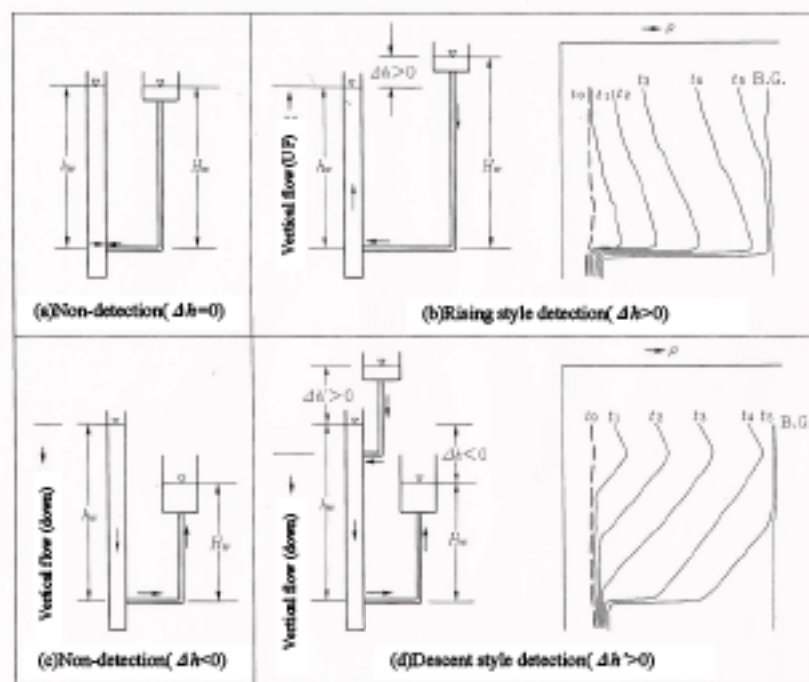


Figure 2.4.3 Principle of groundwater resistivity logging to detect groundwater flow

Set  $\Delta h = H_w - h_w$ , then,

In case-a, when  $\Delta h = 0$ : there is no flow-in from the aquifer to the borehole, hence the existence of the aquifer layer cannot be detected.

In case-b, when  $\Delta h > 0$ : As the groundwater flows into the borehole, and the groundwater layer is detected. If the  $\Delta h$  is not so large, the logging curve becomes wide, and the thickness of the aquifer layer can be detected accurately. When  $\Delta h$  is quite large, the in-flowing groundwater rises a vertical within the borehole which makes the boundary of aquifer layer somewhat fuzzy. Nonetheless, it still allows us to determine the existence of the pressured groundwater.

In case-c, when  $\Delta h < 0$ : As the groundwater in the borehole flows out to the surrounding ground, the existence of the aquifer cannot be detected.

In case-d, when  $\Delta h < 0$ : Although it is similar to the case-c, case-d applies when aquifer layer is detected in the middle of the water level in borehole ( $h_w$ ) indicated in case-b.

## 2.4.7 Interpretation results

Table 2.4.2 presents the interpretation results of groundwater flow based on the groundwater resistivity logging.

In boreholes B00-16 and B05-31, obvious groundwater flow has been detected. Especially in B00-16, the pumping down of the groundwater was very difficult which confirms that an abundant supply of groundwater. Figure 2.4.4 shows the groundwater resistivity logging results in B00-16. The monitoring data and result figures are presented in the Appendix.

Table 2.4.2 Result of groundwater resistivity logging

Location	Borehole Number	Natural water test		Pumping test	
		Zone(m)	Flowing division	Zone(m)	Flowing division
L/S 00	B00-16	11.75-20.00	Groundwater flowing-in	11.75-20.25	Groundwater flowing-in
		20.00	Leakage of groundwater	20.25-20.50	Pressured groundwater
L/S 05	B05-31	23.50-25.00	Groundwater flowing-in	23.50-25.00	Groundwater flowing-in
		28.25	Leakage of groundwater	25.00-34.00	No flowing
L/S 27	B27-24	21.75-22.50	Groundwater flowing-in	22.00-23.75	No flowing
		23.75	Leakage of groundwater	23.75	Leakage of groundwater
L/S 28	B28-10	31.50-38.75	No flowing	31.50-34.00	Groundwater flowing-in
				34.75	Leakage of groundwater
				34.75-38.75	No flowing
	B28-33	—	—	23.00-28.00	No flowing

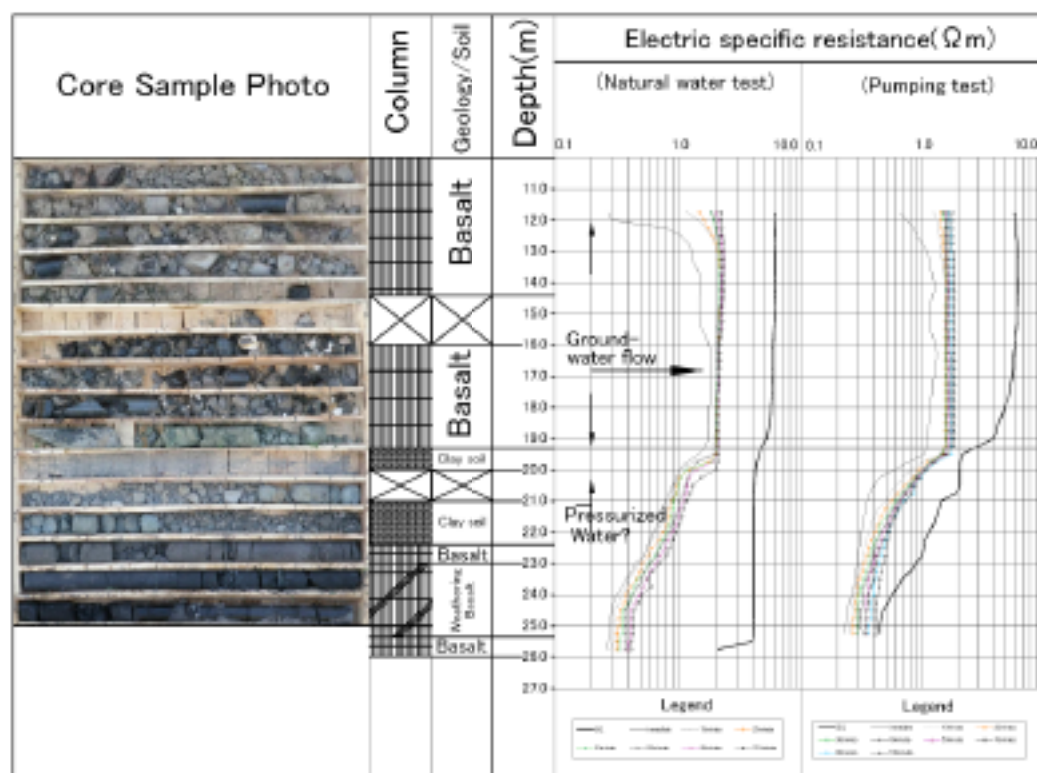


Figure 2.4.4 Groundwater logging (B00-16)

# Chapter 3

---

*Landslide Analysis and Interpretation*



### 3 Landslide Survey

#### 3.1 Cross sectional interpretation

Representative geological cross sections for each selected site are prepared on the basis of the geological features of each landslide block in the previous description. The geological cross sections are displayed in the following figures

##### 3.1.1 LS/00

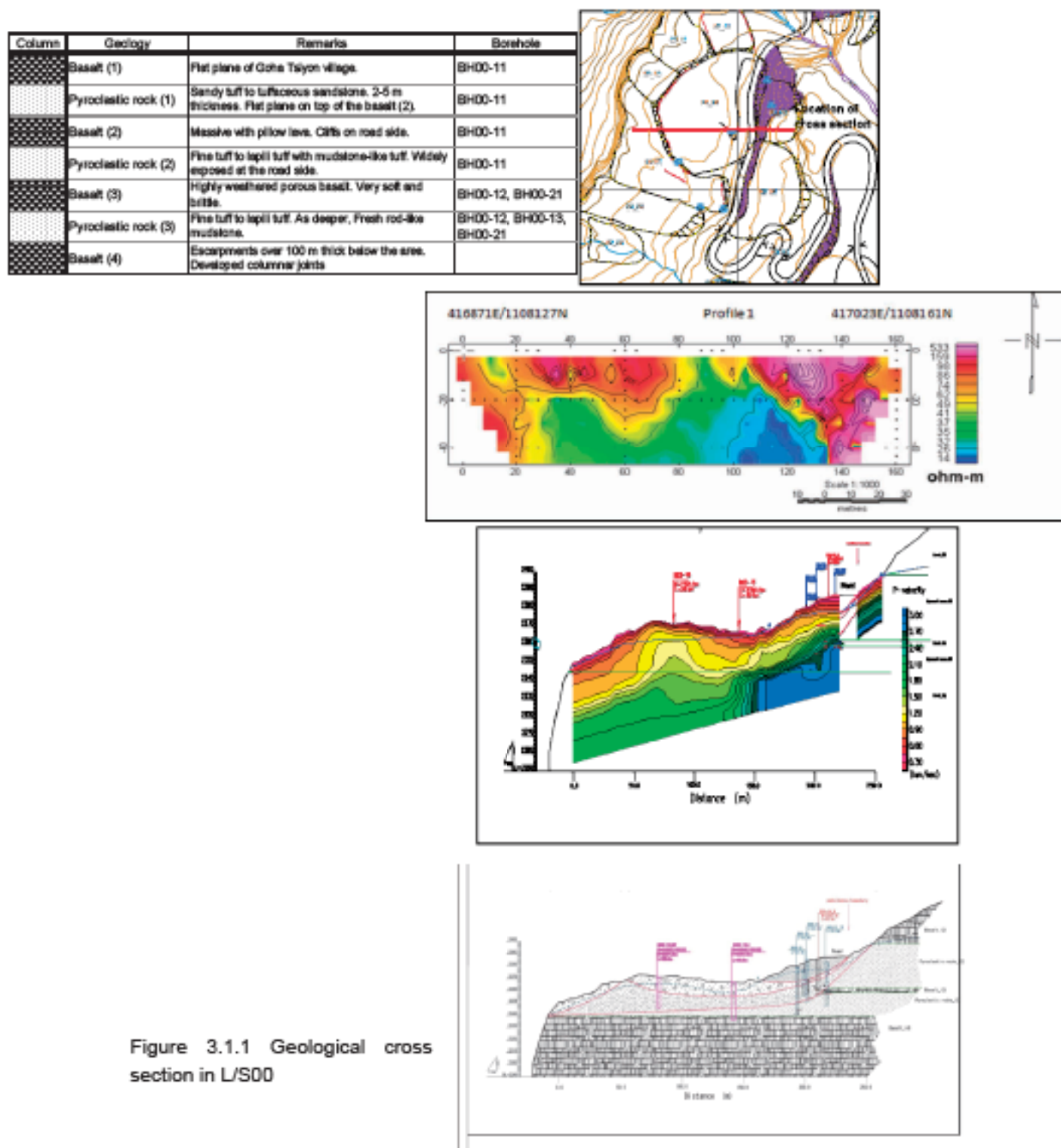






Figure 3.1.1 Geological cross section in L/S00

### 3.1.2 LS/05

Column	Geology	Remarks	Borehole
	Basalt	Massive. The phenocryst is small, like mudstone.	
	Tuff (highly weathered basalt ?)	Sand or mud of soft particles prone to liquefying. A few m thickness.	
	Upper limestone	Thick limestone beds and minor intercalation. Steep slopes and escarpments. Pale grey in color.	BH05-11, BH05-21, BH05-31
	Lower limestone	Thick limestone beds and tuffaceous beds. Gentle slopes. Grey white to white in color.	BH05-12, BH05-22, BH05-32

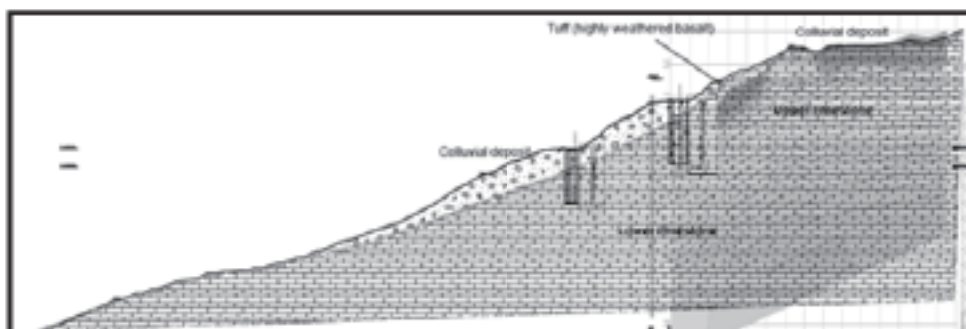
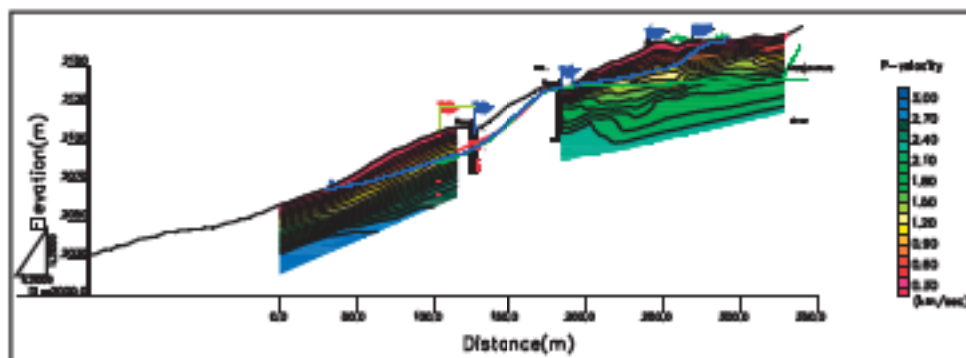
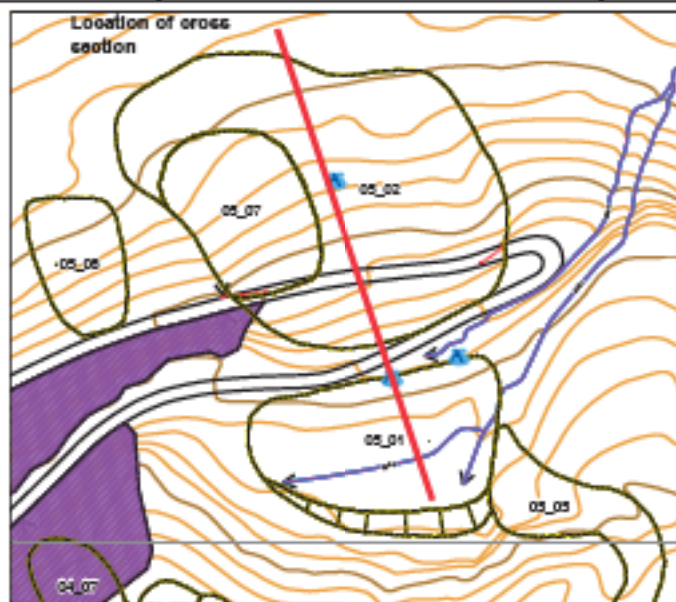




Figure 3.1.2 Geological cross section in LS/05

### 3.1.3 LS/27-28

Column	Geology	Remarks	Borehole
	Limestone	Thick limestone beds and tuffaceous beds. Steep cliff including overhang. Grey white to white in color.	
	Silt and shale	Siltstone and shale with limestone mixed with sliding soil mass. Gentle slope. Landslide forms.	BH27-11,12,21,22,23, BH28-11,21,31,32,41

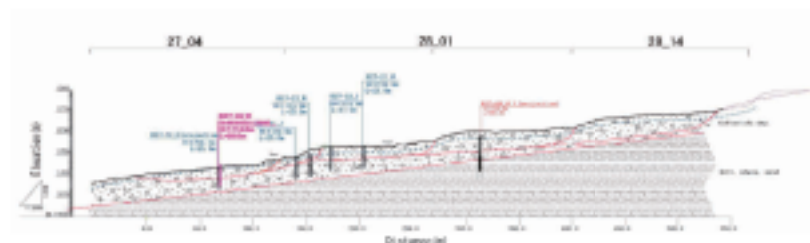
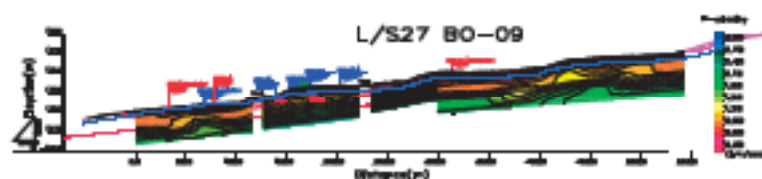
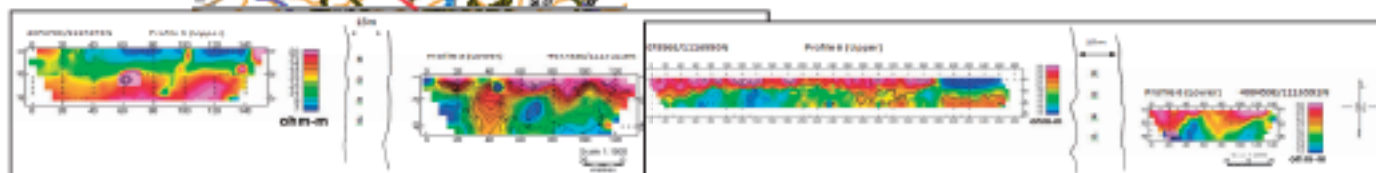


Figure 3.1.3 Geological cross section in L/S27

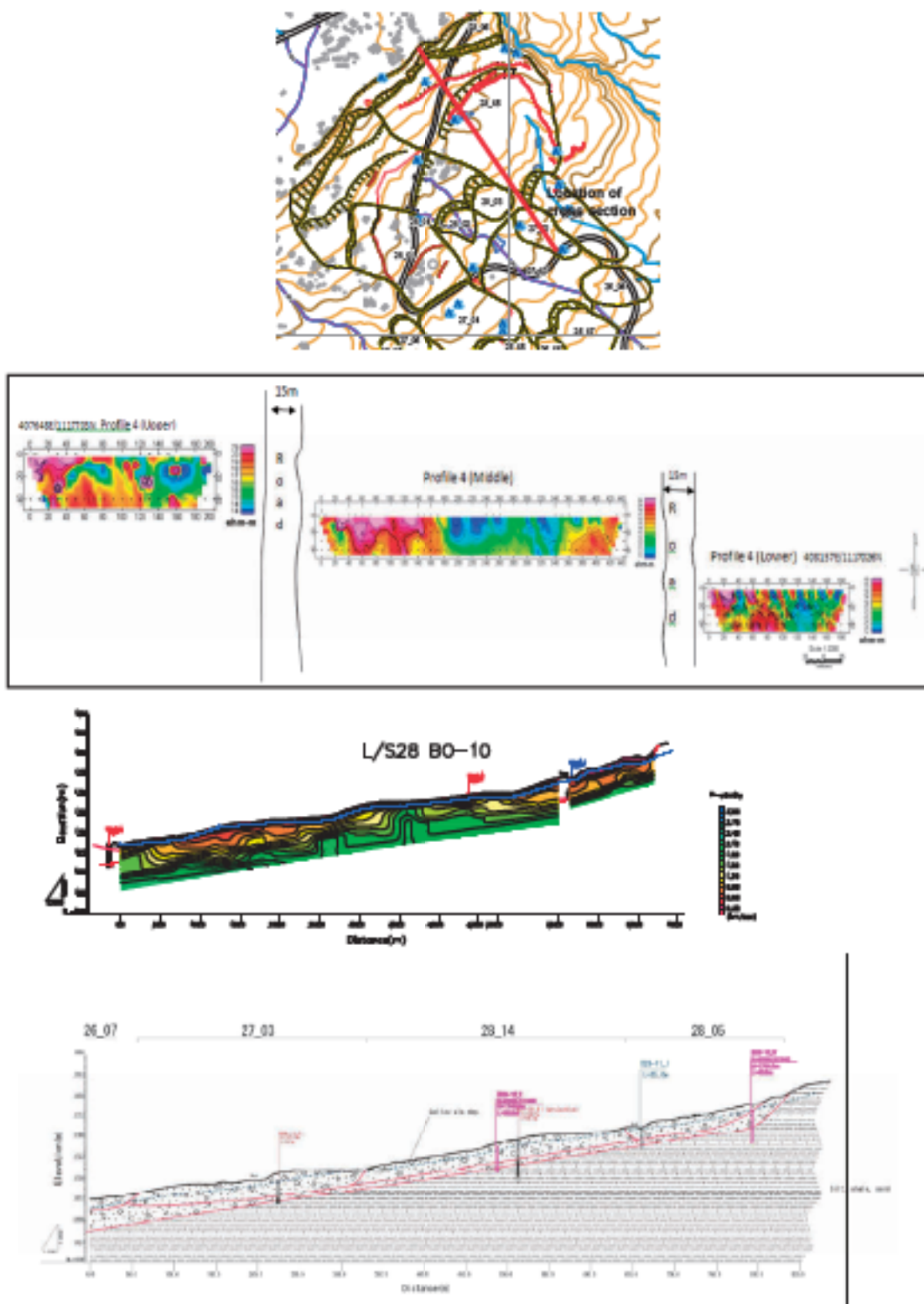


Figure 3.1.4 Geological cross section in L/S28

### 3.2 Monitoring data interpretation

The outline result of the monitoring with the equipment is shown in the following table, and the detailed results are explained below.

Table 3.2.1 Outline of the monitoring results

Location	Extensometer		Borehole extensometer		Borehole inclinometer		Water level meter	
L/S00	EX-1	42.4mm (Compression 26.6mm)	B00-11	0.1mm	B00-12	16.2m	B00-21	-20 to -23m Highest -18.1m
					B00-22	10.5m		B00-16
					B00-15	Single measurement so far		
L/S05	EX-2	45.5mm (Compression 1.9mm)	B05-11	7.1mm	B05-21	6.6m (minute movement:29.8m)	B05-12	-31 to -32m Highest -31.0m
	EX-3	52.8mm (Compression 3.8mm)			B05-22	11.6m (minute movement:28.0m)		B05-31
L/S27	EX-4	61.8mm (Compression 0.9mm)	B27-12	No movement	B27-11	8.0m	B27-21	-22 to -24m Highest -21.9m
	EX-5	201.2mm	B27-13	- 0.3 mm (contraction)	B27-22	15.0m		B27-23
							B27-10	22 to 25 m
							B27-24	21 to 22 m
B27-09	18 meter (out of order since August 2011)							
L/S28	EX-6	312.1mm (Compression 0.1mm)	B28-41	0.1mm	B28-11	14.7m	B28-21	-20m Highest -20.0m
			B28-12	Non				B28-31
					B28-32	25.0m	B28-33	15 to 27 m
							B28-23	26 to 30 m
			B28-10	31 m				

#### 3.2.1 LS/00

At the site only first set of Inclinometer measurement has been possible to take until February 2012. Subsurface displacement is recorded at 16 meter depth (B00-12); direction of displacement is south ward along the slope profile (southward) with considerable secondary westerly (down slope) component. Groundwater level is constant around 11 meter depth from the surface (B00-16) and at 24 meters depth at B00-14. Also recorded at B00-21 is 20 meter deep below the surface. No displacement is recorded at the location of B00-11 extensometer.

### 3.2.2 LS/05

Groundwater table at 22 meter depth is measured with short lived very low spiky variation probably due to instability of sensor (B05-31), around 32 meter deep at B0512 and 35 meter deep at B05-13 also noted. Inclinator data shows maximum of 15 mm/month displacement starting at depth of 13 meter (B05-13). Minor displacement of less than 5mm is recorded at 6 meter depth and 30 meters depth. Displacement of 10 mm maximum per month is found at the site (B05-22). Direction of displacement is towards the valley (northwest) with slight westerly component. Overall major slip zone occurs at 10 meter depth, but shows slowing down tendency from the rainy season data to the dry season.

Cumulative displacement of 8 mm is recorded until February, 2012 from extensometer data showing slowing down activity in the dry season. Sharp drop by 160 mm in displacement is recorded by surface extensometers installed across tension fissures from 40 mm to -120 mm in beginning of January, 2012. No activity has been recorded afterwards until February, 2012 in one of the two surface extensometers installed at the site. The other instrument has not recorded any measurement for the time period of the above displacement due to power shortage (battery).

### 3.2.3 LS/27

Groundwater level recorded was at about 22 meter depth, the depth increased from 21 meter to 22 meter during the dry period (B27-24). About 23.5 and 25 meter depth was recorded at B27-21 and B27-10 sites since October 2011 to February, 2012.

Very slight contraction is recorded 0.3 mm by the borehole extensometer (B27-13); on the other hand extension by about 50 mm was recorded at B27-12 and has since been maintained same value after 6th of September, 2011.

The only measurement of subsurface displacement plane remains to be that of B27-22, at 16 meter depth with 48 mm with major displacement component of south east and secondary component of north east. Slower rate of extension is recorded by surface extensometers across tension fractures, from the beginning of August 2010 to August 2011 a similar smooth and stepped increment (following every rainy season) of the extension is recorded, the trend is still increasing but at lower rate until January, 2012 (N0.5): Similarly a smaller but stepped increment is recorded across another fissure in the same area (N0.4) but has not been recording since November 2011 to February 2012 due to power shortage (Battery).

### 3.2.4 LS/28

A displacement of 32 mm/month is recorded starting from 14 meter deep (B2831) from inclinometer. A gradual rise from 25 meter to 23 meter of depth to groundwater table is recorded between the December 2011 and February 2012 despite the decreasing (almost 0mm) rainfall in the time period (B28-22). A rather rapid drawdown of depth to groundwater table is recorded at another location in the same area (B28-33) where the depth drew down from 16 meters to 26 meters below the surface from mid September, 2011 to February, 2012. On the other hand consistent depth to groundwater table is recorded at 30 meters below the surface (B28-33). Still a gradual drawdown in depth to Groundwater table from 26 meters to 30 meters below the surface is recorded (B28-10) which remains constant

after the first rapid draw down in December 2011. The value remains at 30 meters depth afterwards until February, 2012 with some possibly erroneous spikes associated with system instability of the sensor.

A rapid contraction of the subsurface by 7 mm is recorded by the borehole extensometer in the same area at different location December 2011 to February 2012 (B2842); No significant measurement is recorded at locations of borehole extensometer in the area (B2841) from its installation in September 2010 to February, 2012; measurement from (B2812) indicate 0 mm displacement with a number of very high spiky values which cannot be ascertained to be true or artifacts. Most of the spikes reach 100 to 250 mm in length. An irregular but stepped increments of extension is recorded across one of the major tension cracks in the area (No.6)

### 3.3 Discussions on groundwater flow

To investigate the flowing patterns of groundwater, groundwater logging was conducted in 5 boreholes as listed in Table 3.3.1 using either natural water level method or pumping method. The pumping method can detect any flows of the pressured groundwater located in deep layer, which is difficult to be detected with the natural water level method.

In borehole B00-16, it is obviously detected a pressured groundwater flow existing in the strongly weathered tuff layer at the depth from 19.5m to 20.5m. In the colluvial deposit layer consisting of basalt gravel at the depth from 11.75m to 19.5m, a flowing layer was detected in laminar flow state (Figure 3.3.1). While in borehole B28-10, a flowing of weakly pressured groundwater was detected at the depth from 33.5m to 33.75m where siltstone layer and shale layer is located. Over this flowing layer, a laminar flowing layer was detected in the siltstone layer at the depth from 31.5m to 32.0m (Figure 3.3.2). Totally, in dry season, the groundwater level is located below the colluvial deposit layer, and presents the lowest groundwater level in the slope.

Table 3.3.1 Groundwater flowing investigation result through groundwater logging (in dry season)

Borehole Number	Groundwater level	Situation of the groundwater
B00-16	11.75m	At the depth from 19.5m to 20.5m, pressured groundwater layer existed; At the depth from 11.75m to 19.5m, groundwater flowing was at laminar flow state; Below the depth of 20.5m, groundwater flow became to downward flowing.
B05-31	23.75m	Groundwater has almost been drained out, while at the depth from 23.75m to 25.0m, the groundwater flowing was in a surface water flow state.
B27-24	21.75m	Groundwater has almost been drained out, while below the depth of 21.75m, the groundwater flow became to a downward flowing.
B28-10	31.5m	At the depth from 33.5m to 33.75m, a flowing of weakly pressured groundwater was detected. The groundwater was almost drained out, while at the depth from 31.5m to 32.0m, the flowing existed in a surface water flow state. Below the depth of 33.75m, the groundwater flow became to a downward flowing.
B28-33	23.25m	The groundwater was almost drained out, while at the depth from 23.25m to 23.5m, the flowing existed in a surface water flow state. Below the depth of 32.0m, the groundwater flow became to a downward flowing.



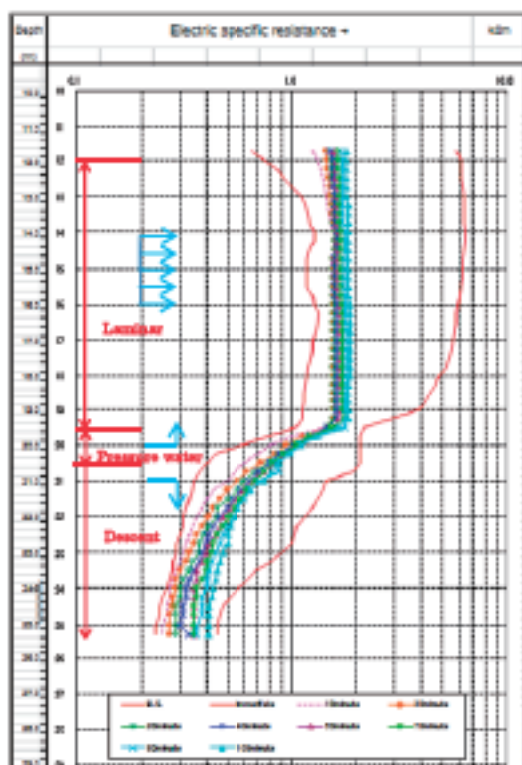


Figure 3.3.1 Result of groundwater logging at borehole B00-16, with the pumping logging method.

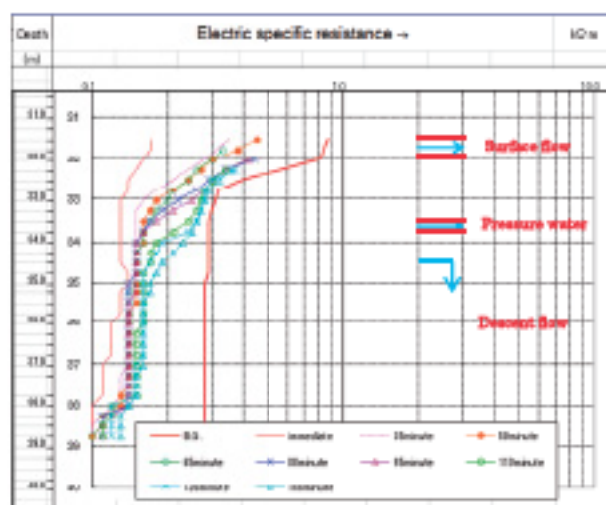


Figure 3.3.2 Result of groundwater logging at borehole B28-10, with the pumping logging method.

### 3.4 Landslide mechanism and hydrogeological structure

#### 3.4.1 Landslide section in each area and their hydrogeological characteristics

In Abay region, from November 2011 to January 2012, additional borehole investigation has been conducted. The investigation has been extended to the outside area of the main road. In this investigation, totally 9 boreholes were executed, i.e., 2 boreholes were conducted in L/S00 area, 2 boreholes in L/S27 area, and 5 boreholes in L/S28 area. With the addition borehole investigation, the landslide mechanism in Abay region became much clearer. Figure 3.4.1 – Figure 3.4.4 show the BO-12 section in L/S00 area, BO-09 section in L/S27 area, BO-13 section and BO-14 section in L/S28. Combined with the investigation on groundwater flowing described in previous section, the following is a summary of the landslide section and hydrogeological characteristics in each area.

##### a. BO-12 section in L/S00 area

From the additional borehole investigation result, it is found that strongly weathered basalt at the depth from 19.0m to 22.6m in borehole B00-15 and weathered tuff layer the depth from 21.0m to 24.0m in borehole B00-16 existed. From the groundwater logging result in B00-16, a pressured groundwater flowing layer was recognized at the depth from 19.5m to 20.5m. Based on these kind of results, it is reasonable to consider that, after passing the basalt and pyroclastic rock, the groundwater formed a flow in the clay layer and weathered tuff layer which is located along the boundary between colluvial deposit and basalt layer, and then became pressured groundwater and infiltrated into the colluvial deposit, finally, formed a inter-stratum water and flow in the colluvial deposits.

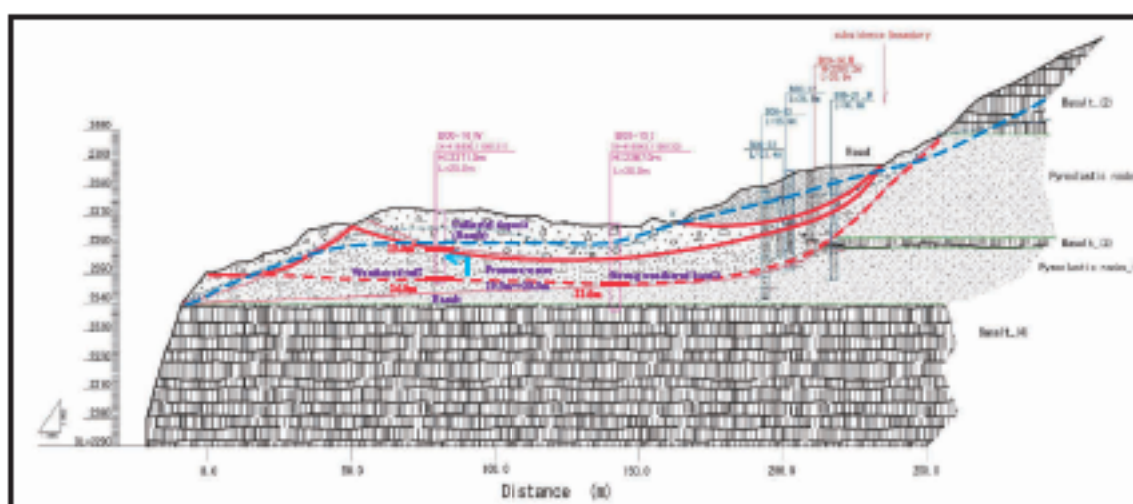


Figure 3.4.1 Landslide section (BO-12 in L/S00 area)

##### b. BO-09 section in L/S27 area

In borehole B27-13, it is found that the depth of the boundary between colluvial deposits containing basalt gravel and the bedrock of siltstone or mudstone layer was 15.0m, and clay layer was located at the depth between 14.0m and 15.0m. While in borehole B27-24, the depth of the boundary between the colluvial deposit containing basalt gravel and bedrock of siltstone was 20.4m. From the situation of the landslide blocks, it is considered that two types of landslide may exist in this area; one is a shallow slide in the shallow colluvial layer, the other is a deep slide along the bottom of the deep colluvial deposit. The groundwater level in borehole B27-24 in dry season was 21.75m, this makes the deep slip surface can always be

kept under the groundwater. Additionally, the groundwater logging result shows a downward flowing existed below the depth of 21.75m. It is estimated that an upward flowing should occur in rainy season. However, the groundwater monitoring result up to now did not show the upward flowing.

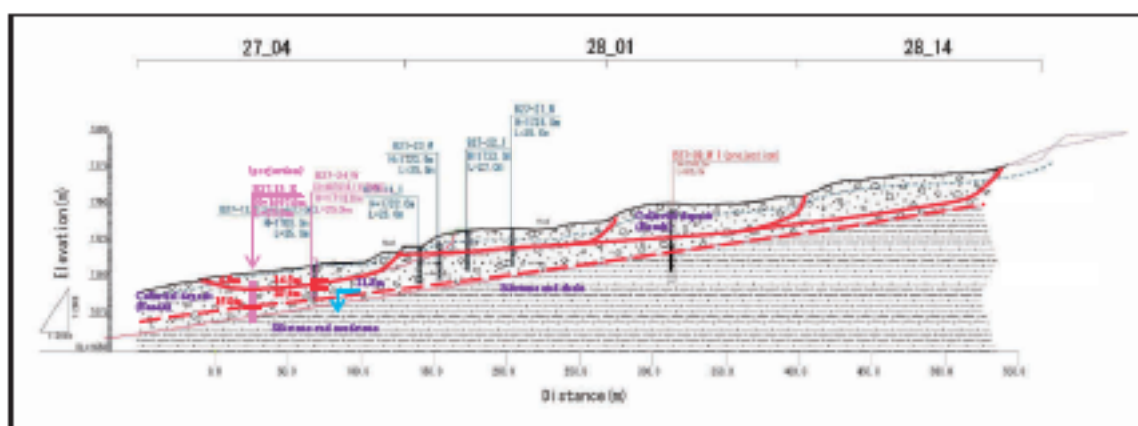


Figure 3.4.2 Landslide section (BO-09 in L/S27 area)

**c. BO-13 section in L/S28 area**

In borehole B28-10, it is found that the depth of the boundary between colluvial deposits containing basalt and limestone gravel and the bedrock of siltstone or shale layer was 28.2m. While in borehole B28-12, the depth of the boundary between the colluvial deposit containing basalt gravel and bedrock of siltstone or mudstone was 25.6m, and weathered mudstone layer were located at the depth between 18.0m and 20.0m, and at the depth between 23.3m and 25.6m. From the landslide block situation, it is also considered that two types of landslide may exist in this area: one is a shallow slide in the shallow colluvial layer, and the other is a deep slide along the bottom of the deep colluvial deposit. The groundwater level in borehole B28-10 in dry season was 31.5m. This makes the deep slip surface can always be kept under the groundwater. Additionally, the groundwater logging result of borehole B28-10 shows a weakly pressured groundwater flowing existed in the siltstone and shale layer at the depth between 33.5m and 33.75m. It may be possible that after passing the weathered siltstone, the groundwater infiltrated into the colluvial deposits mixed with basalt gravels.

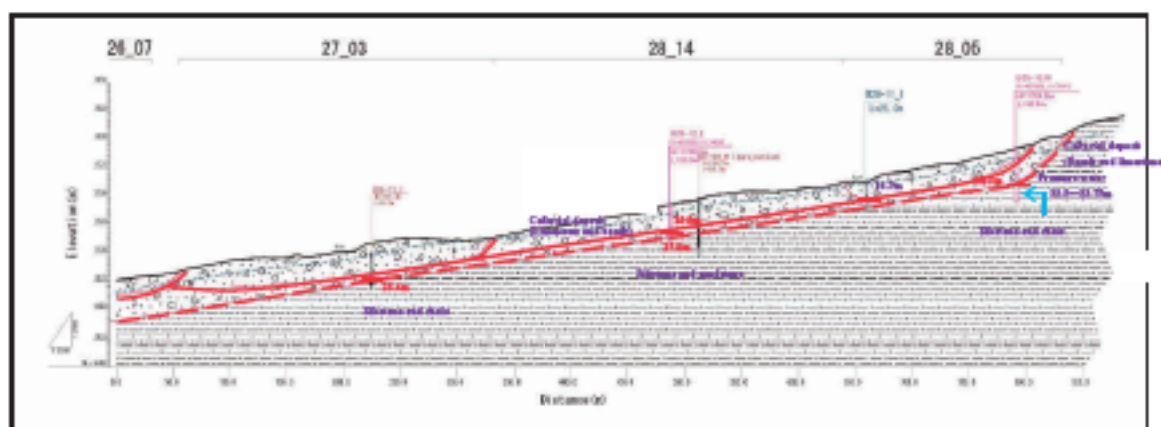


Figure 3.4.3 Landslide section (BO-13 in L/S28 area)

#### d. BO-14 section in L/S28 area

In borehole B28-22, it is found that the depth of the boundary between colluvial deposits and the bedrock of mudstone or siltstone layer was 28.5m, especially the depth of between 17.3m and 17.5m, and the layer between 24.4m and 25.6m are strongly weathered. In borehole B28-33, the depth of the boundary between the colluvial deposit and bedrock of siltstone layer was 24.6m, especially the layer between 18.0m and 19.2m is strongly weathered. In borehole B28-42 the depth of the boundary between colluvial deposits and the bedrock of mudstone or siltstone layer was 18.5m. While the borehole bending occurred at depth 14.5m of borehole B28-11 and depth 10.0m of B28-32. From the landslide block situation, it is considered that two types of landslide may exist in this area, one is a shallow slide in the shallow colluvial layer, and the other is a deep slide along the bottom of the deep colluvial deposit. In dry season, the groundwater level in borehole B28-33 was 23.2m, there always is a water head existing over the slip surface. Additionally, the groundwater logging result shows that there is weak surface water flowing existing at the depth between 23.25 and 23.5m. In this block, the groundwater is an unconfined groundwater, and it infiltrates to the weathered siltstone or mudstone layer.

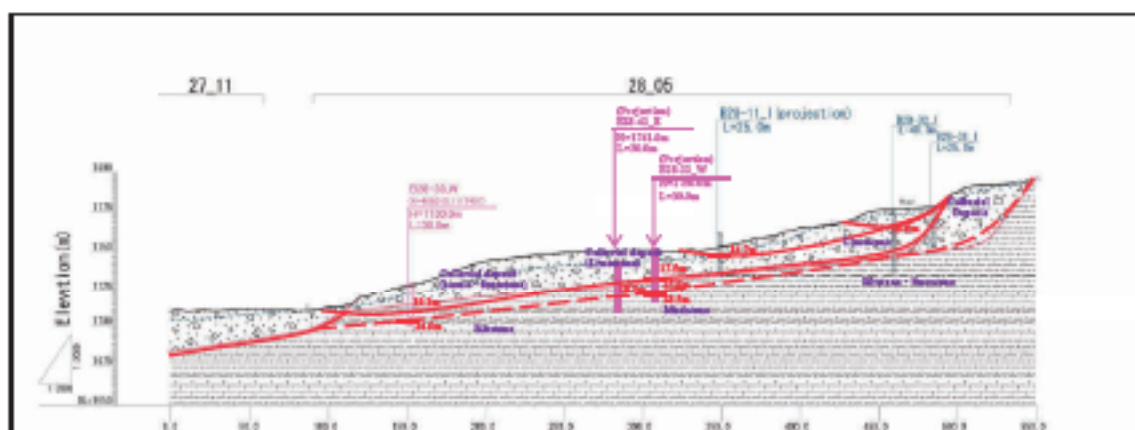


Figure 3.4.4 Landslide section (BO-14 in L/S28 area)

### 3.4.2 Summary of landslide mechanism and future works

Most of the landslides in Abay region occurred in colluvial deposits. Strongly weathered tuff layer or clay layer is located at the boundary between the colluvial deposits and the bedrock of siltstone or mudstone layer, supplying a favorable condition for landsliding. Overall, from the investigation result, it is clarified that under the manifested shallow landslide, there may be a deep-seated landslide, such as a shallow landslide in the colluvial deposits overlaying a deep landslide with slip surface along the bottom of the colluvial deposits. While partly in L/S05 area slip surface was detected in the weathered limestone layer.

Also, the existence of the pressured groundwater has been confirmed in L/S00 area and L/S28 area. It is also confirmed that, beside the vertical infiltration of the rainfall, the groundwater formed a flow along the weathered tuff layer, siltstone layer, mudstone layer after the infiltration to the deep, and infiltrated to colluvial deposit after it becoming to be pressured, and finally flowed in the colluvial deposit layer.

From the extensometer monitoring result in L/S27 and L/S28 areas, it is found that creeping

deformation occurred even besides the rainy season. The possible reason may be the narrow existence of the strongly weathered tuff layer and clay layer at the boundary between the colluvial deposit and bedrock of siltstone and mudstone layer.

In rainy season, the landslide deformation became active. This may be explained by the increasing of pore-water pressure caused by rainfall. However, in the monitoring up to now, the water level increasing has seldom been recorded. It is expected for further data accumulation in rainy season. In the process of executing landslide countermeasure works such as groundwater drainage work, it is very necessary to continue the groundwater level monitoring, each kind of landslide deformation monitoring, even for the effect evaluation of the groundwater drainage work.

# Chapter 4

---

*Technical Transfer*

## 4 Technical Transfer

### 4.1 Groundwater resistivity logging equipment

This technical transfer involved two days of practical training. On the first day 19 December, 2011, an expert of geophysical exploration/analysis from the JICA Study Team explained functions of and procedures for operating groundwater resistivity logging equipment at GSE office. This was necessary for understanding groundwater flows at the site.

On the second day, 20 December, 2011, involved demonstrations by the expert and on-the-job-training (OJT) at the Ethiopian Water Technology Center (EWTEC). The counterparts used the equipment for various measurements, and then analyzed the results.

The groundwater resistivity logging equipment is important for monitoring the movement of groundwater. This data is vital for deciding where to locate a drilling point. A list of participants and some pictures are as follows.

Table 4.1.1 Participants list on 2days seminar (19 and 20 December, 2011)

No.	Name	Organization	Date
1	Getnet Mewa	GSE	19 December
2	Sisay Alemayehu	GSE	19, 20 December
3	Alayu Atnafu	GSE	19, 20 December
4	Zulfa Abdurahman	GSE	19, 20 December
5	Tadesse Lema	GSE	19, 20 December
6	Ezra Tadesse	GSE	19, 20 December
7	Brook Abel	GSE	19, 20 December
8	Daniel Kassaye	GSE	19, 20 December
9	Kefale Tilahun	GSE	19, 20 December
10	Yewubnesh Bekele	GSE	19, 20 December
11	Samuel Molla	GSE	19, 20 December
12	Habtamu Eshetu	GSE	19, 20 December
13	Genet Assefa	GSE	19, 20 December
14	Debebe Kifle	GSE	19, 20 December
15	Mulugeta Kinfu	EWTEC	20 December
16	Hussen Endre	EWTEC	20 December
17	Megignet Abeje	EWTEC	20 December
18	Abubeker Yasin	EWTEC	20 December
19	Haftamu Tadesse	EWTEC	20 December
20	Jemila Shemsu	EWTEC	20 December
21	Hafta Mulu	EWTEC	20 December
22	Tilahun Sileshi	EWTEC	20 December
23	Zerihun Gobena	EWTEC	20 December
24	Demiss Miiku	EWTEC	20 December
25	Endale Merru	EWTEC	20 December
26	Endress	EWTEC	20 December
27	Yoji Kasahara	JICA Study Team	19, 20 December
28	Takeshi Kuwano	JICA Study Team	19, 20 December
29	Yosuke Yamamoto	JICA Study Team	19, 20 December
30	Masami Takahata	JICA Study Team	19, 20 December



Figure 4.1.1 Photos of the in-house seminar



Figure 4.1.2 Photos of the demonstration of the groundwater resistivity logging at EWTEC



## 4.2 Laboratory soil test

### 4.2.1 General

GSE has experience in geological resource mining and geochemical investigations. Also, GSE has enough equipment for geochemical analysis, e.g.: instruments to measure weight, hydraulic content, grading composition. However, they do not have appropriate equipment to investigate landslide mechanisms because they have less research experience on landslide disasters. Therefore, it is a good time for GSE to set up essential equipment for landslide analysis. For progressing skills of GSE to prevent landslides, the following equipment is immediately needed to measure physical properties which reveal landslide mechanisms and decide the countermeasures.

### 4.2.2 Laboratory soil test equipment

#### a. Procured experimental equipment

1) Direct shear strength test machine	1 set
2) Compressive strength test machine for soil	1 set
3) One-dimensional consolidation test machine	1 set
4) Cone penetrometer for liquid limit of soil consistency test	1 set
5) Compressive strength test machine for rock	1 set

#### b. Soil survey to mitigate landslides

The causes of landslide generation can be divided into basic factors and inducing factors. The former is mainly geology, landforms, water behavior in the ground and vegetation. The latter is rainfall events and earthquakes. When the basic factors coincide with the inducing factors, landslides are generated. If there is no basic factor on a hillslope, the possibility of landslide generation surely decreases. This is why, depending on the type of location, landslides may or may not occur during the same rainfall event. The basic factors strongly affect landslides occurrence. Therefore, it is very important and essential for landslide prevention to investigate the basic factors of landslide generation.

As previously mentioned, geology, landforms, water behavior in the ground and vegetation are the key basic factors of landslide generation. The common element in these factors is soil. Bedrock changes into soil by weathering and various landforms arise in the process from bedrock into soil. Water behavior in the ground and vegetation facilitate this process. The characteristics of soil generated from bedrock by weathering increase the probability of landslide generation. Mass movement occurs easily in loose soil. Also, soil holding much water flows downward easily. Compacted soil is tough and it does not move easily. In other words, clarifying the soil characteristics of a potential landslide area can make the timing and mechanisms of landslides clearer. The soil characteristics are determined by the physical values measured through various soil tests. (Figure 4.2.1)

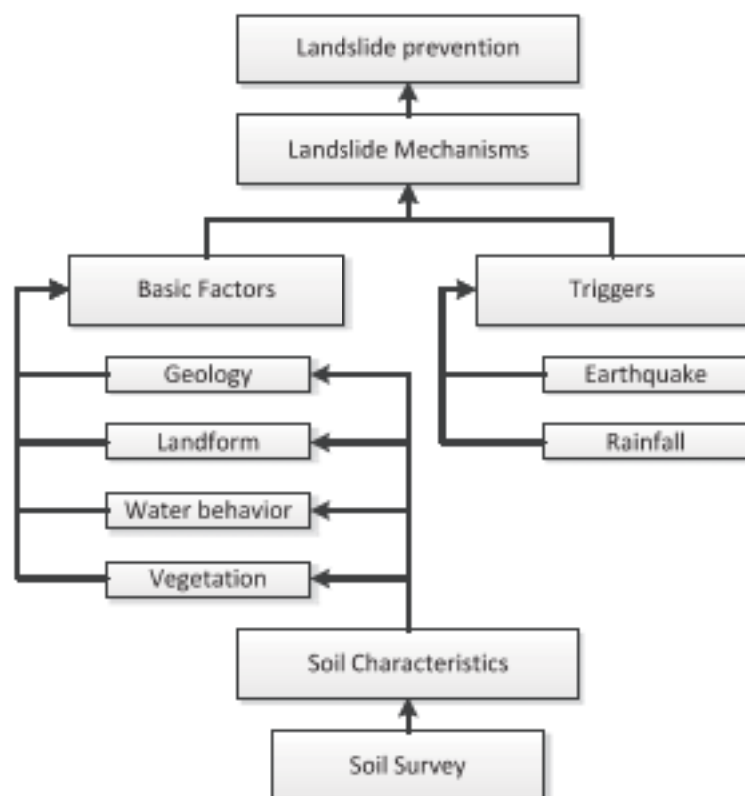


Figure 4.2.1 Flowchart of soil survey for landslide prevention

### c. Various soil tests and physical results for landslide countermeasures

On a hillslope, landslide generation can be expressed by the following equation,

$$\text{Sliding force downward} > \text{Resisting force against shearing force}$$

Therefore, landslide generation can be prevented by increasing the resisting force against shearing force. Resisting force can be explained by soil cohesion,  $c$ , and angle of internal friction,  $\phi$ . These physical values are called the strength parameter of soil and they are measured directly by direct shear strength test with the following machine.

#### 1) Direct shear strength test

Direct shear strength test clarifies the physical values which are vertical pressure,  $\sigma$ , shear strength,  $\tau$ , cohesion,  $c$ , angle of internal friction,  $\phi$ . Procedure of this test is; 1) setting a soil sample in a box which can be separated up and down, 2) sliding the upper part of box by applying vertical pressure on it, 3) shearing a soil sample and measuring vertical pressure,  $\sigma$ , and shear strength,  $\tau$ , when shear failure occurs, 4) repeating same tests for several samples with various vertical pressures. Cohesion,  $c$ , and angle of internal friction,  $\phi$ , can be calculated from the coordinate of vertical pressure,  $\sigma$ , and shear strength,  $\tau$ , which



Figure 4.2.2 Direct shear strength test

values were measured directly by the tests. The values that were plotted in the coordinate, x-axis :  $c$ , y-axis :  $\phi$ , draw a straight line of a linear equation which was composed by cohesion,  $c$ , and angle of internal friction,  $\phi$ . The equation is as below,

$$\tau = \rho \tan \phi + c \quad (4-1)$$

Cohesion,  $c$ , and angle of internal friction,  $\phi$ , can be found from this equation. This equation is called "Coulomb failure criteria".

Resisting force against shearing force varies depending on the behavior of pore water in soil. Thus, it is needed to investigate how the mechanical characteristics of soil are changed by the behavior of pore water in soil. Therefore, compressive strength test and consolidation test are carried out by focusing on behavior of pore water to replicate main slip surface condition of landslides.

### 2) Compressive strength test

Compressive strength test is carried out to estimate the resisting force against shearing force of cohesive soil under undrained condition which is called undrained shear strength,  $s_u$ , by using compressive strength of the soil,  $q_u$ . The equation to calculate  $s_u$  is as below,

$$s_u = q_u / 2 \quad (4-2)$$

In this test, a soil sample is compressed up and down until the sample is destroyed. Also, compressive strength,  $q_u$ , can be calculated from amount of compression,  $\Delta H$ , and compressing force,  $P$ , which are measured by the test. The compressive strength is interpreted as resisting force against shearing force by soil mass movement. This test is carried out on undisturbed materials like clay or accumulated alluvial soil near roads at a site.



Figure 4.2.3 Compressive strength test machine for soil

### 3) One-dimensional consolidation test machine

Soil is composed of soil grain and pore water or gas. Consolidation is the phenomenon of that low permeable soil loses its volume with discharging pore water for a longer time by a load. Consolidation test measures the decrement of the volume. Because saturated cohesive soil has low permeability and much pores in soil, it takes time to discharge pore water and the decrement of volume is high. Therefore, the amount of consolidation becomes large in saturated cohesive soil. In addition, discharged water might cause high pore water pressure in a closed system like a main slip surface in ground. Also, the water increases weathering of bedrock. These facts influence the condition of main surface slip caused by landslide and they are related to the landslide mechanisms. High pore water pressure lifts up the soil mass of landslide body and decreases resisting force against shearing



Figure 4.2.4 One-dimensional consolidation test machine

force of landslide. To avoid such phenomena that increase the extent of a landslide, appropriate countermeasures are determined using the results of consolidation tests. The decrement of consolidation and the velocity which were measured from consolidation test are related to soil plasticity. Therefore, soil consistency test is needed.

#### 4) Cone penetrometer for liquid limit of soil consistency test

Behavior of soil mass is changed by the water content; “solid” - “semisolid” - “plastic body” - “liquid”. This change is called soil consistency. Liquid limit is the water content ratio when a soil changes into liquid from plastic body. Soil consistency test is based on the relationship between moisture content and the penetration of a cone into the soil sample under controlled conditions. Simple liquid limit test without a cone penetrator is less-accurate. Therefore, this test using a cone penetrator is important to be measured accurately. Cone penetrometer enables the determination of liquid limit to be performed. When the water contents ratio of soil is closing to plastic limit, the soil is stable. But soil closing to liquid limit is unstable and it becomes easy to flow like liquid by a small shock. Thus, liquid limit test shows when soil becomes and behaves like liquid.



Figure 4.2.5 Cone penetrometer

At main slip surface of landslide, it can be estimated that bedrock is becoming argilliferous soil or clay-rich rock due to weathering by water. Such soil and rock continue to hold water from rainfall at the main slip surface. They flow like liquid at main slip surface when they exceed the liquid limit. At the same time, the soil and rock lose their shear strength as bearing resistance in slope ground. Because the soil mass exists above the main slip surface, the soil mass also flows out with argilliferous soil or clay-rich rock. It means that a landslide will occur. The results of the test with this device can be used to estimate the timing when soil and rock lose the shear strength at main slip surface above their liquid limit and make soil mass slipping downward.

#### 5) Compressive strength test

This machine measures the strength of a rock by compressing the rock up and down. Because the strength of a rock is related to landslide occurrence along with soil shear strength, the strength value of rock can be used for analyzing landslide mechanism. This test is carried out to basalts and limestones of Abay Gorge.

All of the above soil tests are used to determine soil cohesion,  $c$ , and angle of internal friction,  $\phi$ , at the main slip surface of a landslide. Those physical values,  $c$  and  $\phi$ , are used for the landslide stability analysis. Then, landslide countermeasures, designs and construction, are planned with reference to the factor of safety which is calculated from the analysis. Therefore, the investigation through various soil tests is important for preventing landslides.



Figure 4.2.6 Compressive strength test machine for rock

### 4.2.3 Application for landslide analysis

In this section, several examples between soil survey results and landslide feature in Japan are introduced. The following table shows the cohesion,  $c$ , and the angle of internal friction,  $\phi$ , in various landslide situations.

Table 4.2.1 Cohesion and angle of internal friction of various landslides

Sample	Cohesion (kPa)	Angle of internal friction ( $^{\circ}$ )	Unit weight (g/cm <sup>3</sup> )	Sampling depth (GL-m)
Landslide A	4.0	32.9	2.3	4.0
Landslide B-1	25.1	32.7	-	34.2
Landslide B-2	0.0	26.2	2.7	28.4
Landslide B-3	13.5	31.6	2.7	47.4

Landslide A: Dip slope. Geology is siltstone which holds a few centimeters of tuff and volcanic glasses. Tuff layer is loose.

Landslide B-1, 2, 3: Landslides B-1, B-2 and B-3 are the same landslide. But the sampling depth is different. Dip slope. Geology is alternation of sand and sandy mud which contains some conglomerates. The landslide is located 200 – 400 meters above sea level. Slope length and width of the landslide are 650m and 450m respectively. Movement distance is about 100m. Shearing bedrock is progressing in landslide B-1. Landslide B-2 is just a main slip surface. Clay content is high in landslide B-3.